A 4800 BPS GTFM MODEM

PART 1– ANALYSIS AND SIMULATION

Prepared for
Communications Research Center
Shirley Bay, Ontario

By

W.P. LeBlanc — Co-investigator
J.K. Cavers — Principal Investigator

July 1986

RELEASABLE

UNIVERSITY:	Simon Fraser
TITLE:	A 4800 BPS GTFM modem part 1--Analysis and simulation part 2--Implementation and performance tests
DOC CR NO:	DOC-CR-SP-86-039
DSS CONTRACT NO:	36100-5-0088
DOC SC. AUTH.:	Brian Bryden
AUTHOR:	W.P. LeBlanc & J.K. Cavers
REPORT DATE:	July 1986

A 4800 BPS GTFM MODEM
PART ONE- ANALYSIS AND SIMULATION

Prepared for
Communications Research Center
Shirley Bay, Ontario

Under DSS Contract Number
06ST.36100-5-0088
(OST85-00238)

By
W.P. LeBlanc Co-investigator
J.K. Cavers Principle Investigator

Faculty of Applied Science
School of Engineering Science
Simon Fraser University
Burnaby, B.C. V5A 1S6

July 1986

A 4800 BPS GTFM MODEM

Part 1- ANALYSIS AND SIMULATION

APPENDICES

A. The Viterbi Algorithm

1. INTRODUCTION

This document reports on the development of a modem designed to operate at 4800 bps over an MSAT channel. The prototype implementation gives excellent performance, within measurement error of the values predicted by simulation.

MSAT system design is organized around 5 kHz slots, to be used by narrowband voice terminals, both ACSSB and digital. In particular, the digital terminal combines a vocoder and a modem, with its original design calling for 2400 bps and MSK modulation. Simon Fraser University developed a prototype modem for the digital terminal under previous contracts from CRC, using a DSP (digital signal processing) chip for the implementation, and obtained very good BER performance.

The quality of vocoded speech at 2400 bps, however, is a controversial issue, even with the unit developed by CRC. Continuing work at CRC has led to a 4800 bps vocoder with greatly improved voice quality. This prompted the search for a 4800 bps modem which would still operate with the 5 kHz MSAT slot. The problem given to SFU was this: select a modulation scheme with constant envelope at 4800 bps with 5 kHz channel spacing, and devise a receiver to give acceptable performance in noise and adjacent channel interference.

The results are satisfying. We met MSAT requirements; in fact the performance is better than any results quoted in the literature for practicable demodulation methods. Moreover, the results time scale to demonstrate the possibility of 24 kbps with standard land mobile 25 kHz channel spacing. Finally, the implementation rests on a general purpose DSP chip, so it does not suffer from problems of drift, aging, and other analog ailments.

In summary form, our main technical results are:

1. We investigated two incoherent detection structures - discriminator and differential - using simulation. The structures were similar: front end filter for adjacent channel and out of band noise rejection, detector, post detection lowpass (except for the differential detector) and Viterbi algorithm.
2. We designed the front end and post detection filters simply by running an adaptive filter, in the worst case noise and adjacent channel interference conditions, to minimize mean squared error.
3. The presence of the front end filter caused blurring of the post detector eye diagrams, and in some cases, an outright separation of the levels. We compensated by approximating the eyes with an experimentally derived encoding polynomial in the Viterbi Algorithm.
4. In the discriminator detector, the 6 level eye (nominal 5) was less smeared than the nominal 3 level eye. We found that a 4 state VA used on the 6 level eye gave between 0.8 and 1.2 dB better performance than a 2 state VA on the 3 level eye.
5. The discriminator detector was 0.4 dB worse than a result in the literature for a 2 state VA which was unhampered by the tight front end filter we need for adjacent channel rejection.
6. The differential detector with its 6 level eye (nominal 5 level) and 4 state VA was 0.4 to 0.6 dB better than the equivalent discriminator detector, and 0.7 to 1.1 dB better than both the best previously reported results in the literature for this class of detector and optimum incoherent TFM with an 8 bit window.
7. Degradation due to parameter error for the 4 state differential detector is: 0.60 dB for 2 per cent frequency offset; 0.4 dB for sample time error of 0.125 symbol duration; 0.4 dB for both adjacent channels

13.5 dB higher than the desired channel.

8. The DSP chip loading of the differential detector was also better than the differential detector, so we adopted it.

2. SYSTEM MODEL

2.1 Continuous Phase Modulation

The class of continuous phase constant envelope modulation techniques known as Continuous Phase Modulation (CPM) is known for its compact spectral properties and good error rate performance. The class of full response CPM systems encompasses those modulation techniques in which the phase is a continuous function of time, and the instantaneous frequency variation of the transmitted signal depends only on the transmitted data symbol in that interval. It is important to note that the instantaneous phase may, and usually does, depend on preceeding data symbols. Minimum Shift Keying (MSK) and Continuous Phase Frequency Shift Keying (CPFSK) belong to the class of full response CPM. If we allow controlled intersymbol interference, in essence correlation between adjacent symbols, we obtain the class of CPM termed partial response CPM. Generalized Tamed Frequency Modulation (GTFM) and Gaussian Minimum Shift Keying (GMSK) belong to the class of partial response CPM systems. (GTFM and GMSK are to be discussed in sections 2.2 and 2.3 respectively).

For the general CPM system, the transmitted signal (following the notation in [1] is:

$$s(t,\underline{\alpha}) = \sqrt{2P}\cos(2\pi f_c T + \phi(t,\underline{\alpha}) + \phi_0)$$

where

$$\underline{\alpha} = \ldots\ \alpha_{-2},\alpha_{-1},\alpha_0,\alpha_1,\alpha_2\ \ldots$$

is the infinitely long sequence of m-ary uncorrelated data symbols, PT is the symbol energy (E_b), T is the symbol period, f_c is the carrier frequency, ϕ_0 is an arbitrary constant phase shift, and

$$\phi(t,\underline{\alpha}) = 2\pi h \int_{-\infty}^{t} \sum_{i=-\infty}^{\infty} \alpha_i g(\tau - iT)\,d\tau$$

where h is the modulation index, and g(t) is defined as the frequency pulse.

For the most part m, the number of symbols in the alphabet is unconstrained, but for GMSK and GTFM is constrained to be two (binary).

In complex envelope notation:

$$s(t,\underline{\alpha}) = \sqrt{2P}\ \mathrm{Re}[v(t)\exp(j2\pi f_c T+\phi_o)]$$

where $v(t) = \exp(j\phi(t,\underline{\alpha}))$

Defining the phase pulse as the integral of the frequency pulse (g(t)):

$$q(t) = \int_{-\infty}^{t} g(\tau)d\tau \qquad \lim_{t\to\infty} q(t) = 1/2$$

Thus:

$$\phi(t,\underline{\alpha}) = 2\pi h \sum_{i=-\infty}^{\infty} \alpha_k q(t-kT)$$

By truncating the phase pulse to L symbols, a CPM modulator may be realized.

2.2 Generalized Tamed Frequency Modulation

Generalized Tamed Frequency Modulation (GTFM) belongs to the class of partial response CPM systems, with modulation index h = 1/2. The frequency pulse is defined (figure 2.2.1) as the cascade of a three tap transversal filter with a low pass filter satisfying the Third Nyquist criterion.

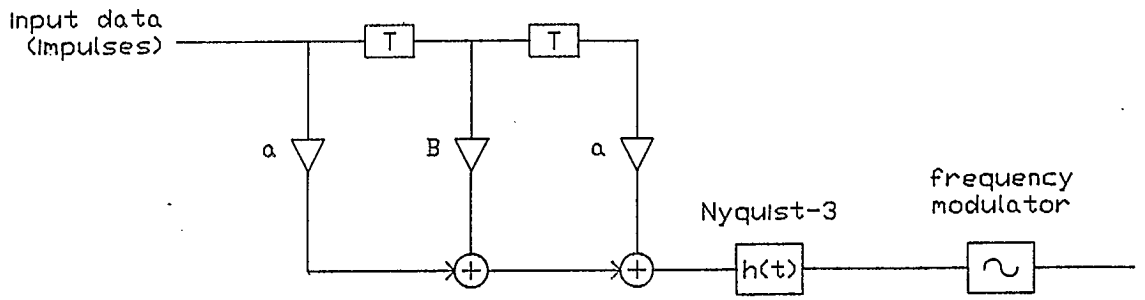

Figure 2.2.1

We have:

$$g(t) = F^{-1}(G(f)) \qquad (F^{-1} \rightarrow \text{inverse fourier transform})$$

$$G(f) = K \cdot S(f)H(f)$$

S(f) is the frequency response of the three tap transversal filter defined by:

$$S(z) = a \cdot z^{-1} + B + a \cdot z$$

where $2a + B = 1$

Thus:

$$S(f) = B + 2a \cdot \cos(2\pi fT)$$

H(f) is a low pass filter with impulse response satisfying the Nyquist-3 criterion. A Nyquist-3 filter can be written:

$$H(f) = W(f)/\text{sinc}(fT) \qquad |f| \leq 1/2T$$

where w(t) satisfies the first Nyquist criterion.

The class of pulses having the spectral raised cosine characteristic satisfies the Nyquist-1 criterion.

That is:

$$W(f) = \begin{cases} 1 & 0 \le |f| \le (1-r)/2T \\ (1-\sin(\pi T(f-1/2T)/r))/2 & (1-r)/2T \le |f| \le (1+r)/2T \\ 0 & \text{otherwise} \end{cases}$$

where r is called the roll-off parameter.

With these definitions:

$G(f) = K(B + 2a\cdot\cos(2\pi fT))W(f)/\text{sinc}(fT)$,

$g(t) = F^{-1}(G(f))$,

$q(t) = \int_{-\infty}^{t} g(\tau)d\tau$ and where K is chosen such that:

$\int_{-\infty}^{\infty} g(t)dt = 1/2$

The possible phase shifts of the carrier during the mth bit period can be expressed as:

$$\phi_m = \phi(mT,\underline{\alpha}) - \phi((m-1)T,\underline{\alpha})$$

$$\phi_m = h\pi(a\alpha_{m-1} + B\alpha_m + a\alpha_{m+1})$$

That is, the correlative encoding rule is due only to S(z) since h(t) is a Nyquist-3 pulse.

By manipulating B, and r we compromise spectral efficiency versus bit error rate (BER) performance. Each particular B,r combination is referred to as GTFM(B,r) in the literature. For example GTFM(0.50,0.0) is just Tamed Frequency Modulation (TFM) and GTFM(0.62,0.36) has been found to be near optimum in terms of reducing the BER and still maintaining a compact spectrum (see section 3.5). (The phase and frequency pulse for GTFM(0.62,0.36) and for TFM is shown in figure 2.2.2 and 2.2.3).

The transmitted power spectrum was computed using the Welch method [26]. A Hanning window was used to pre-window the complex envelope (8

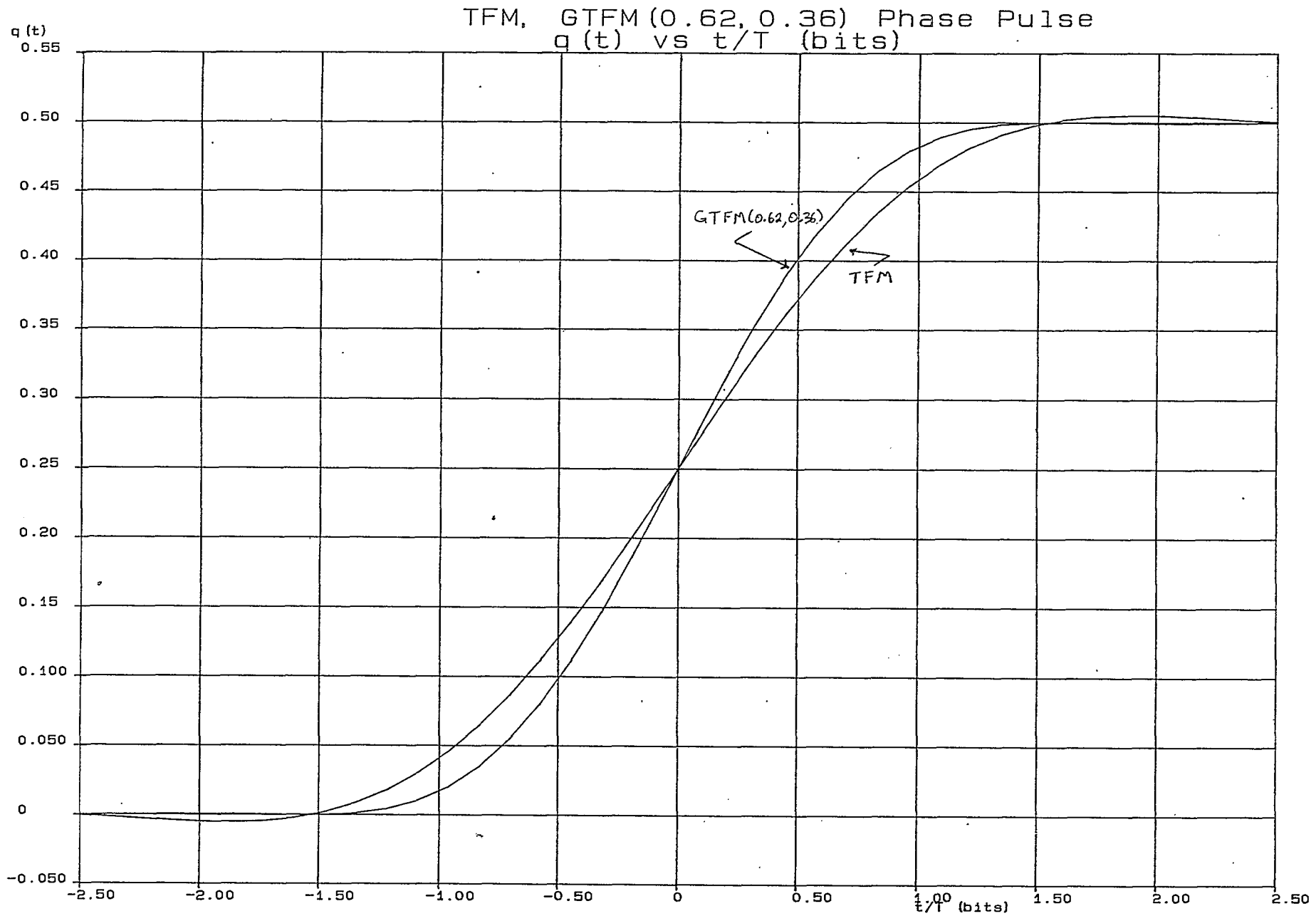
TFM, GTFM(0.62, 0.36) Phase Pulse
q(t) vs t/T (bits)
q(t)
0.55
0.50
0.45
0.40
0.35
0.30
0.25
0.20
0.15
0.100
0.050
0
-0.050
GTFM(0.62,0.36)
TFM
-2.50
-2.00
-1.50
-1.00
-0.50
0
0.50
1.00
1.50
2.00
2.50
t/T (bits)

Figure 2.2.2

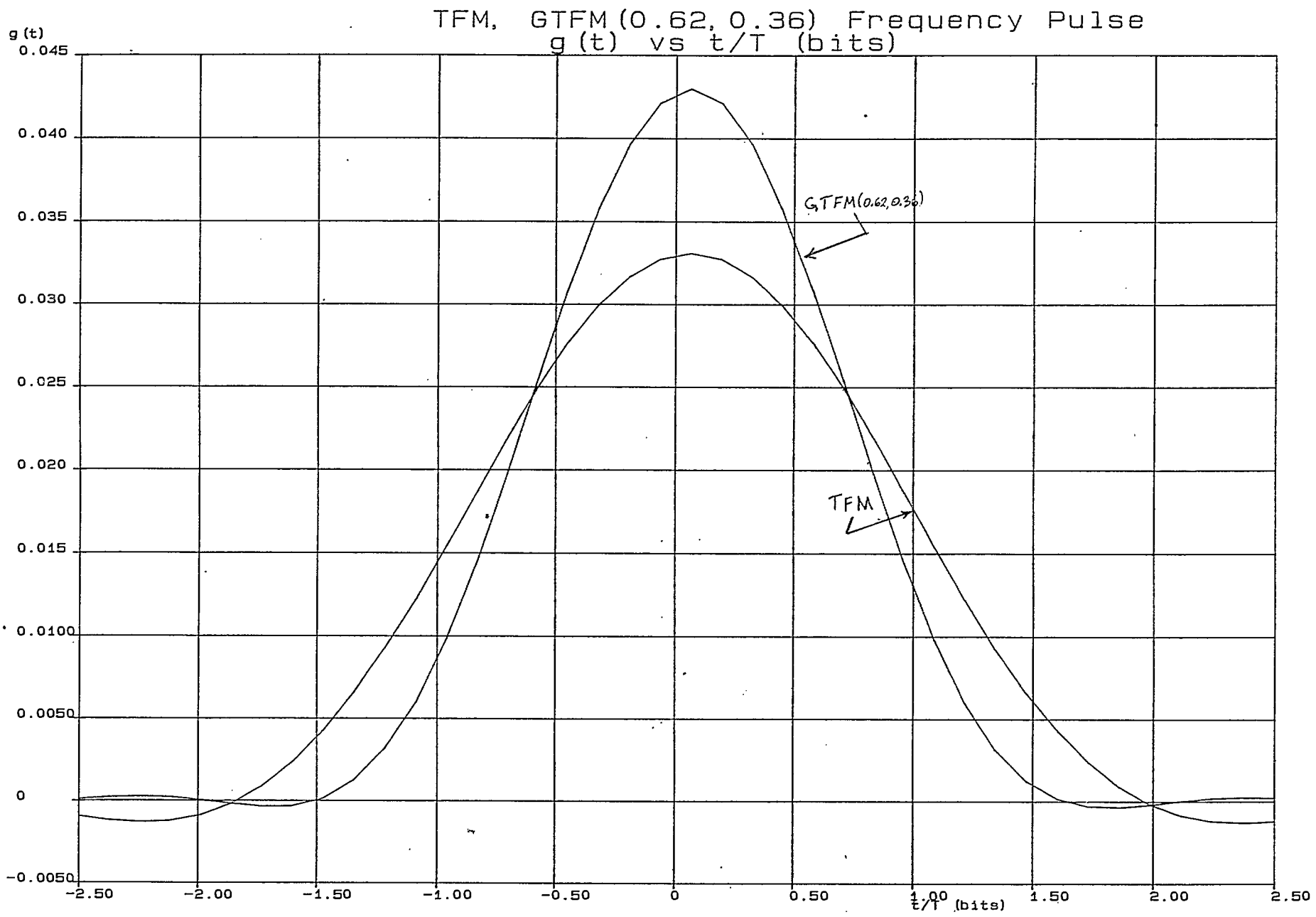
TFM, GTFM(0.62, 0.36) Frequency Pulse
g(t) vs t/T (bits)
g(t)
0.045
0.040
0.035
0.030
0.025
0.020
0.015
0.0100
0.0050
0
-0.0050
-2.50
-2.00
-1.50
-1.00
-0.50
0
0.50
1.00
1.50
2.00
2.50
t/T (bits)
GTFM(0.62,0.36)
TFM

Figure 2.2.3

samples per bit) prior to the M point (M=2048) Fast Fourier Transform (FFT). By repeating the above process K times and averaging the results, (K=512) a good estimate of the power spectral density can be made. The power spectrum of GTFM with various B,r combinations and the reference curve (MSK), is shown in figure 2.2.4. A larger K would further reduce the variance evident in the estimated power spectral density.

The fractional inband power ratio expressed as the ratio of inband power to total transmitted power was computed by summing over the band of interest, and dividing this by the total transmit power, (sum over the whole fourier transform). That is we compute:

$$\sum_{k=0}^{N} \Phi_{vv}(k) / \sum_{k=0}^{M/2} \Phi_{vv}(k)$$

The fractional inband power ratio for various (B,r) combinations is shown in figure 2.2.5. We observe that for GTFM(0.62,0.36) approximately 99.7% of the power is contained in a 1/T (4.8 kHz) band. For MSK, (with no transmit filtering), 99.7% of the power is contained in a 2/T (9.6 kHz) band. Thus, 4.8 kbps GTFM(0.62,0.36) should fit comfortably within a 5 kHz channel.

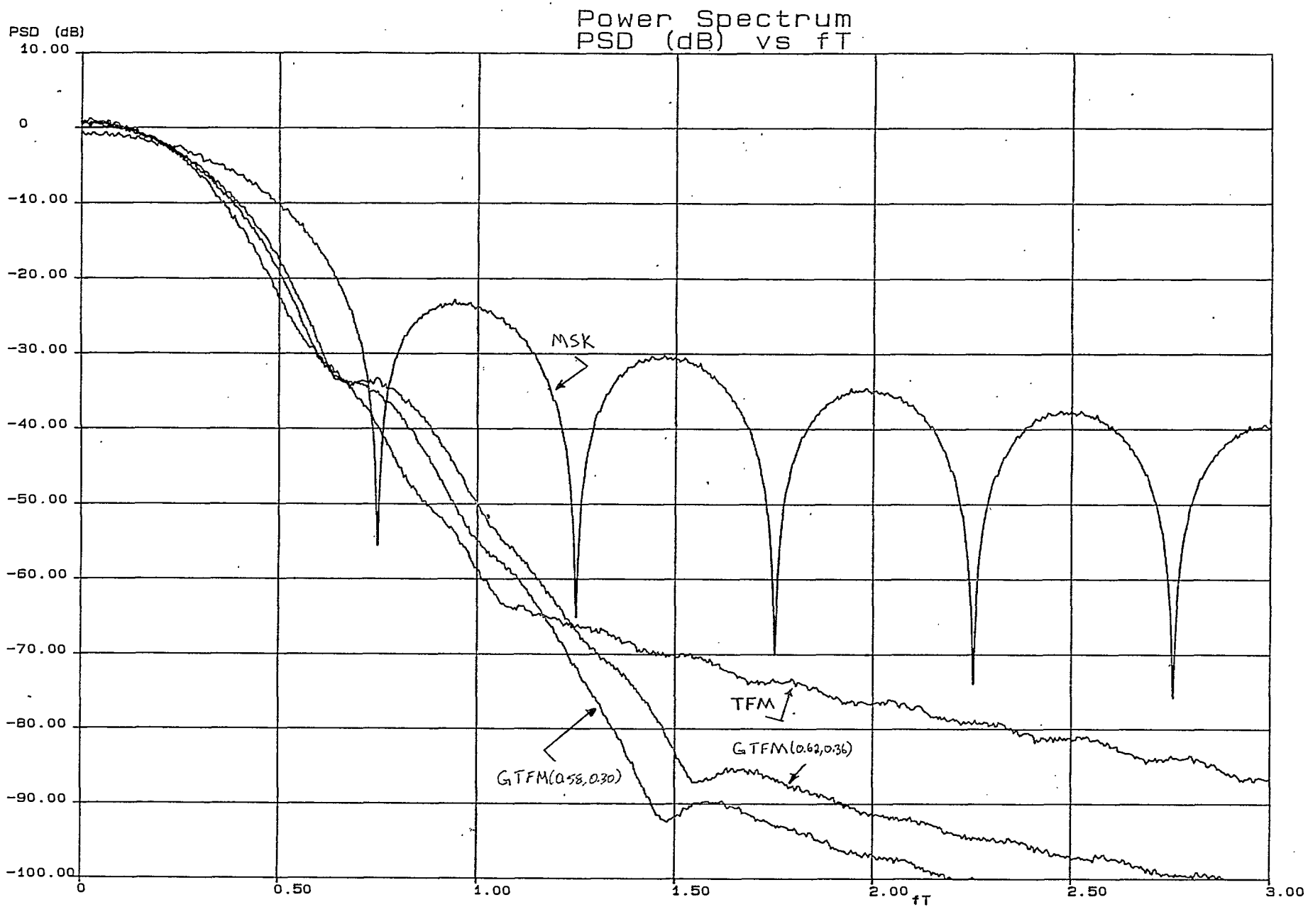
Power Spectrum
PSD (dB) vs fT
PSD (dB)
10.00
0
-10.00
-20.00
-30.00
-40.00
-50.00
-60.00
-70.00
-80.00
-90.00
-100.00
0
0.50
1.00
1.50
2.00
2.50
3.00
fT
MSK
TFM
GTFM(0.62,0.36)
GTFM(0.58,0.30)

Figure 2.2.4

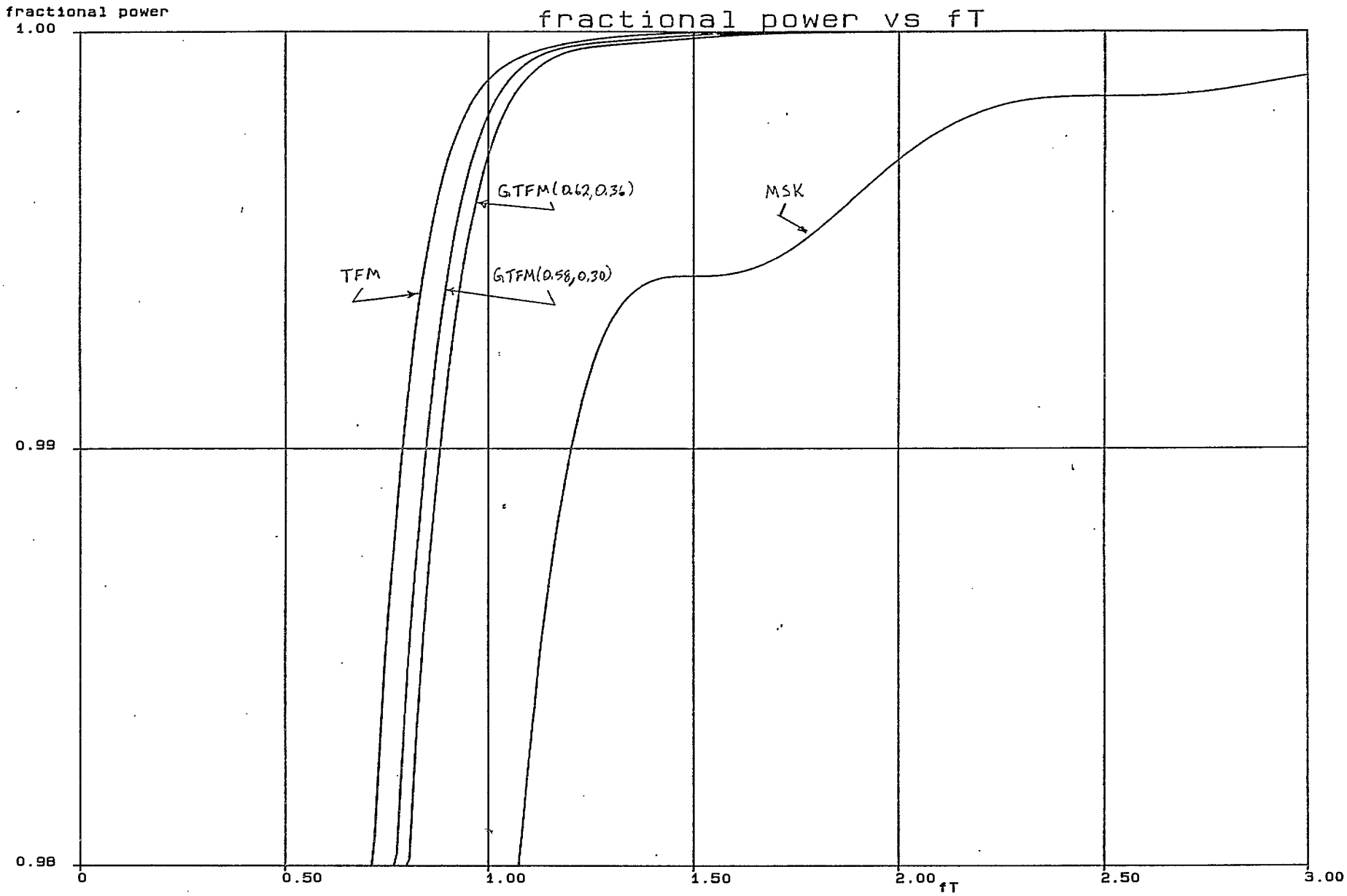
fractional power vs fT
fractional power
1.00
0.99
0.98
0
0.50
1.00
1.50
2.00
2.50
3.00
fT
GTFM(0.62,0.36)
MSK
TFM
GTFM(0.58,0.30)

Figure 2.2.5

2.3 Gaussian Minimum Shift Keying

Gaussian Minimum Shift Keying (GMSK) is an extension of the well known minimum shift keying (MSK), or more accurately, differentially encoded MSK. In GMSK the NRZ data is first low pass filtered before being applied to an FM modulator, with modulation index h = 1/2 (figure 2.3.1).

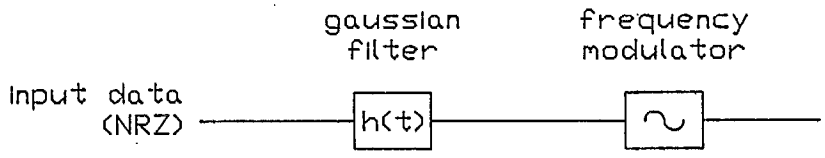

Figure 2.3.1

The low pass filter has a gaussian impulse response, and consequently a gaussian frequency response.

In our CPM model:

$$g(t) = K\overline{\Pi}(t/T) * h(t)$$

where

* denotes convolution,

$$\overline{\Pi}(t/T) = \begin{cases} 1 & |t| \le T/2 \\ 0 & \text{else} \end{cases}$$

K is chosen such that $\int_{-\infty}^{\infty} g(t)dt = 1/2$,

$$h(t) = \sigma \cdot \exp(-(\sigma t/T)^2)/\sqrt{\pi},$$

$$\sigma = 2\sqrt{2\pi}\, B_n T$$

where B_nT is the 3 dB cutoff frequency (equivalent noise bandwidth normalized to the bit rate):

$B_nT = \sqrt{(4\pi/\ln(2))}BT$ where BT is the 3 dB bandwidth

It can easily be shown that:

$$g(t) = K \cdot Q(\sqrt{2} \cdot \sigma(-1/2 - t/T)) - K \cdot Q(\sqrt{2} \cdot \sigma(1/2 - t/T))$$

$$\text{where } Q(x) = 1/\sqrt{2\pi} \int_x^{\infty} \exp(-y^2/2)dy$$

Thus, we arrive at our phase pulse defined as:

$$q(t) = \int_{-\infty}^{t} g(t)dt, \quad q(\infty) = 1/2$$

In the literature GMSK with premodulation filter bandwidth BT is referred to as GMSK(BT). GMSK(0.20) and GMSK(0.25) are the most common. The phase and frequency pulses of GMSK(0.25) and GMSK(0.20) are shown in figures 2.3.2 and 2.3.3. The power spectrum (computed as in section 2.2) of GMSK for various BTs is shown in figure 2.3.4, and the fractional inband power ratio for various BT combinations is shown in figure 2.3.5.

The correlative encoding rule for the instantaneous frequency (GMSK) extends over an infinite number of bits, since the gaussian pulse never truly decays to zero. Thus, this ad hoc method of generating a phase pulse would seem to be inferior to the well defined GTFM. However, for all practical purposes the phase pulse extends only over a finite number of bits. GMSK(0.27) and GTFM(0.62,0.36) are almost identical in terms of phase pulse, frequency pulse, transmitted power spectrum and fractional inband power ratio, (figures 2.3.6-2.3.9). Thus, it would appear that there is little difference between choosing GTFM(0.62,0.36) or GMSK(0.27).

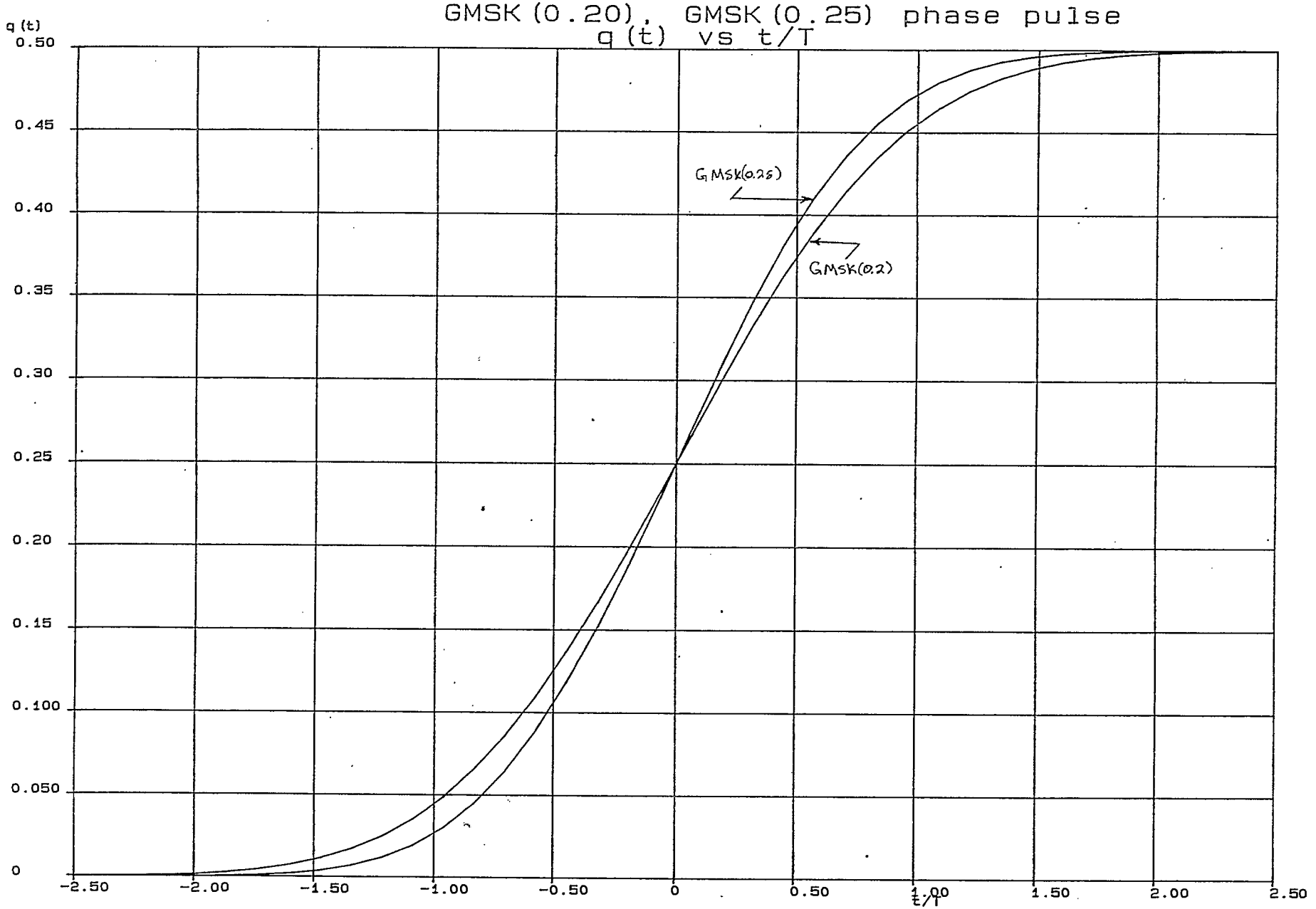
GMSK (0.20), GMSK (0.25) phase pulse
q (t) vs t/T
q (t)
0.50
0.45
0.40
0.35
0.30
0.25
0.20
0.15
0.100
0.050
0
GMSK(0.25)
GMSK(0.2)
-2.50
-2.00
-1.50
-1.00
-0.50
0
0.50
1.00
1.50
2.00
2.50
t/T

Figure 2.3.2

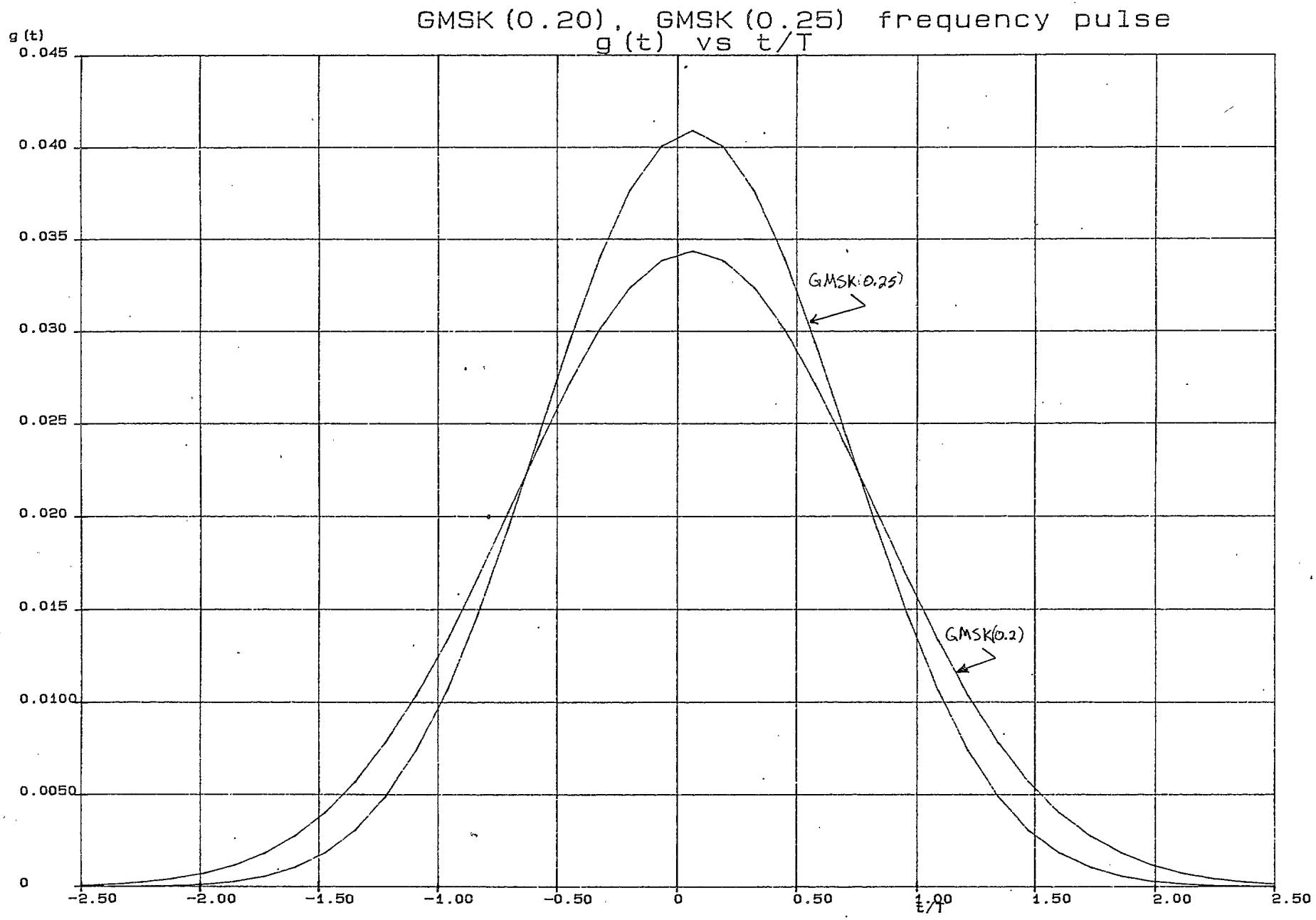
GMSK (0.20), GMSK (0.25) frequency pulse
g (t) vs t/T
g (t)
0.045
0.040
0.035
0.030
0.025
0.020
0.015
0.0100
0.0050
0
GMSK(0.25)
GMSK(0.2)
-2.50
-2.00
-1.50
-1.00
-0.50
0
0.50
1.00
1.50
2.00
2.50
t/T

Figure 2.3.3

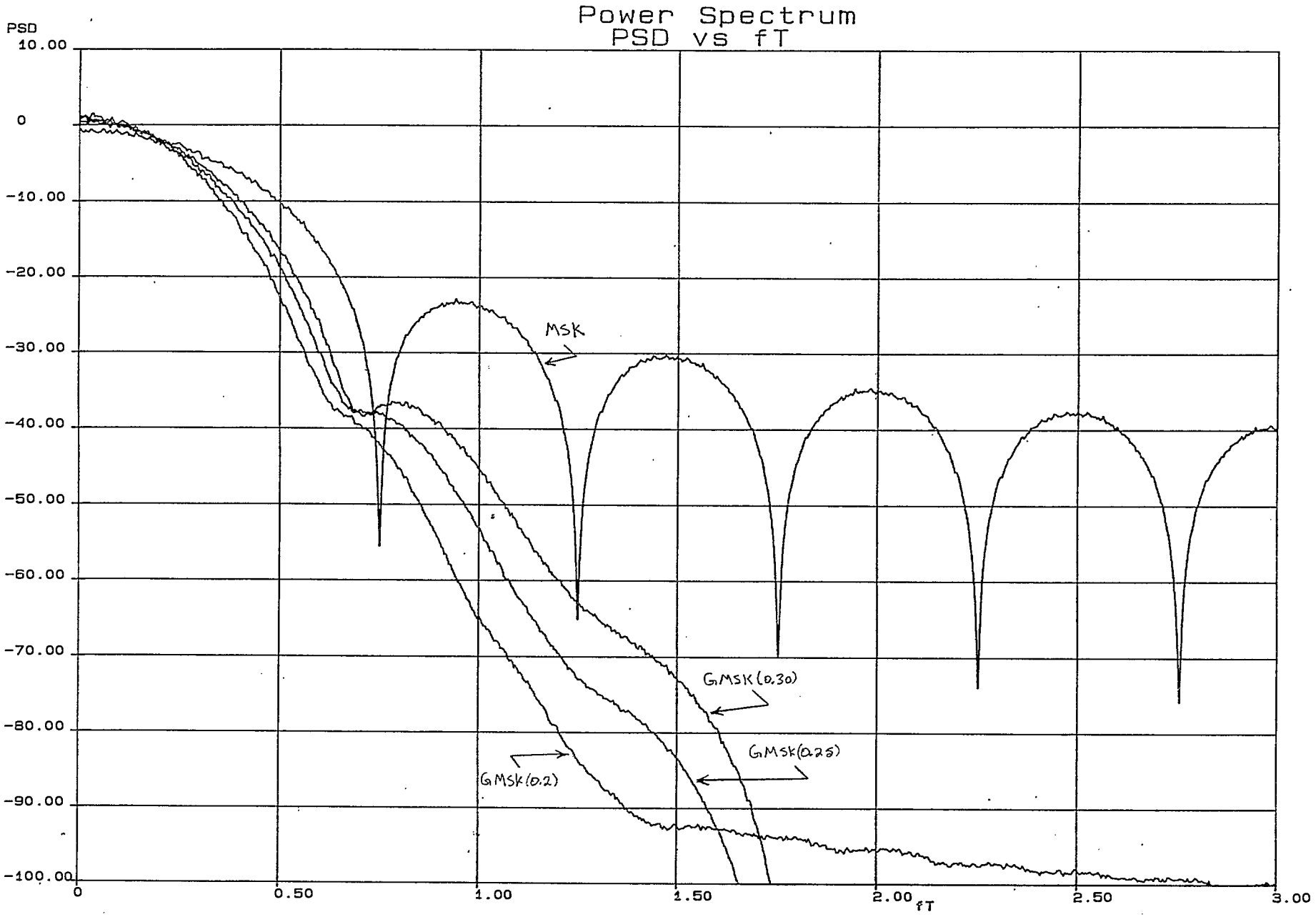
Power Spectrum
PSD vs fT
PSD
10.00
0
-10.00
-20.00
-30.00
-40.00
-50.00
-60.00
-70.00
-80.00
-90.00
-100.00
0
0.50
1.00
1.50
2.00
2.50
3.00
fT
MSK
GMSK(0.3α)
GMSK(0.2s)
GMSK(0.2)

Figure 2.3.4

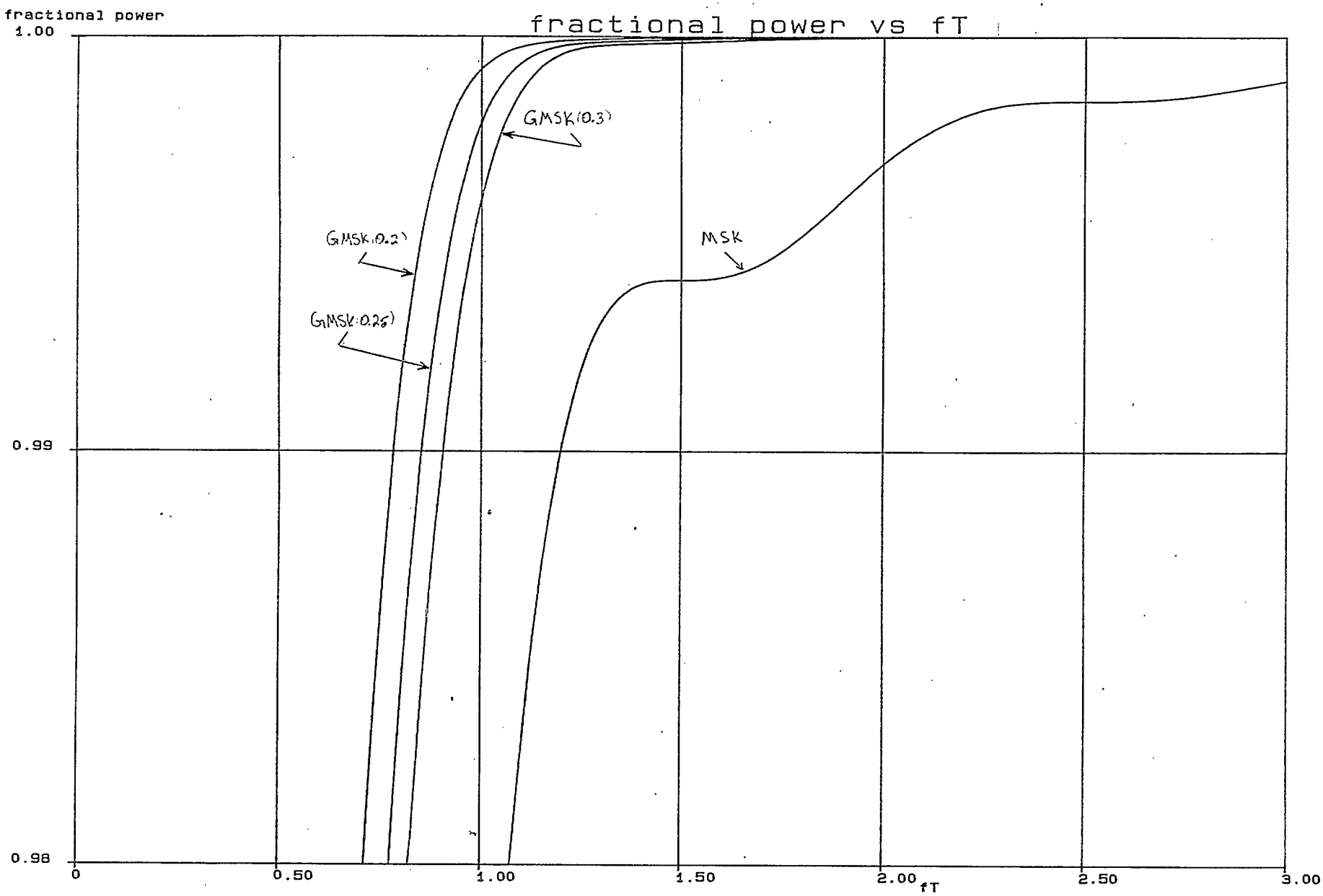
fractional power
fractional power vs fT
1.00
0.99
0.98
GMSK(0.3)
GMSK(0.2)
GMSK(0.25)
MSK
0
0.50
1.00
1.50
2.00
2.50
3.00
fT

Figure 2.3.5

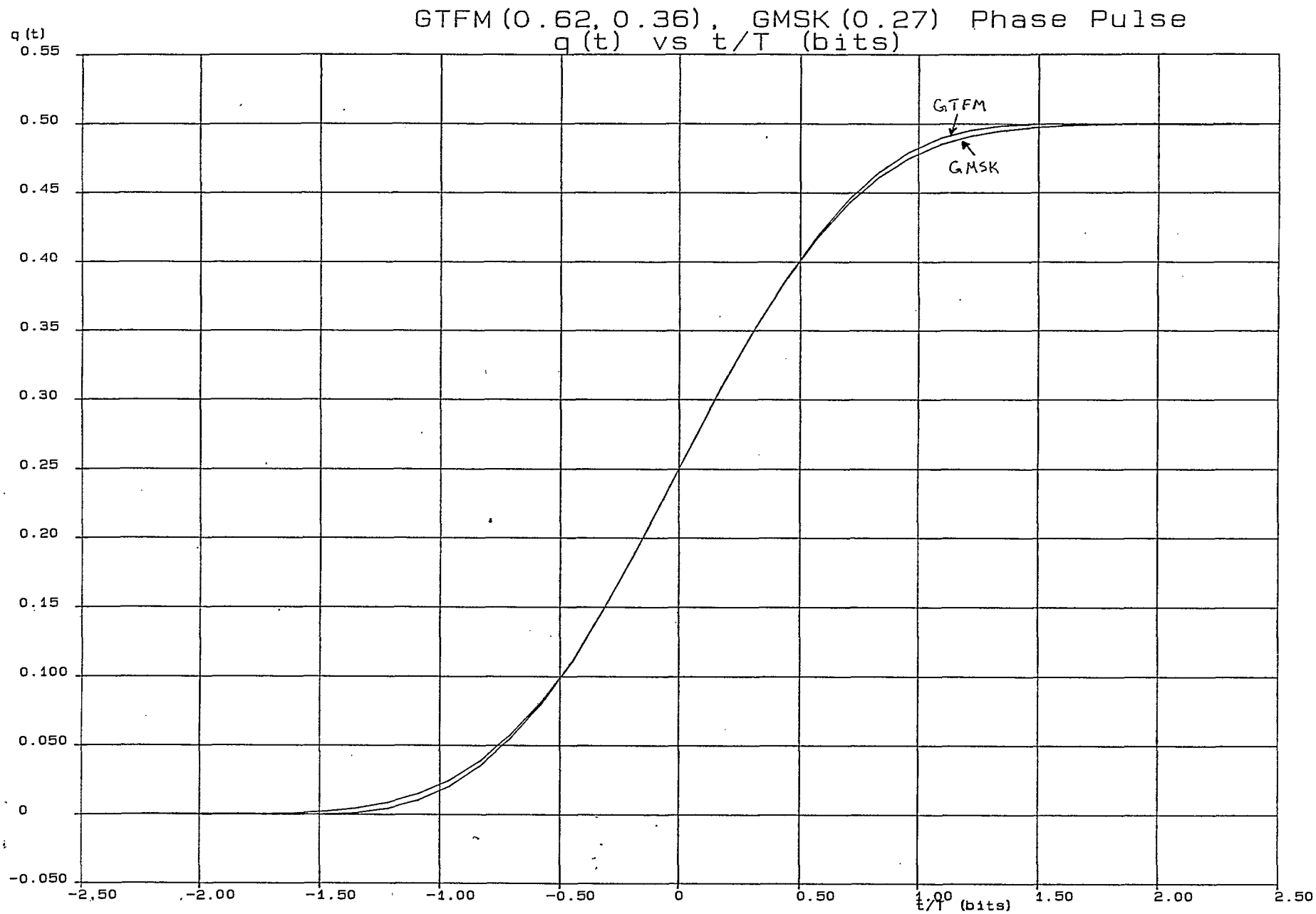
GTFM (0.62, 0.36), GMSK (0.27) Phase Pulse
q (t) vs t/T (bits)
q (t)
0.55
0.50
0.45
0.40
0.35
0.30
0.25
0.20
0.15
0.100
0.050
0
-0.050
GTFM
GMSK
-2.50
-2.00
-1.50
-1.00
-0.50
0
0.50
1.00
1.50
2.00
2.50
t/T (bits)

Figure 2.3.6

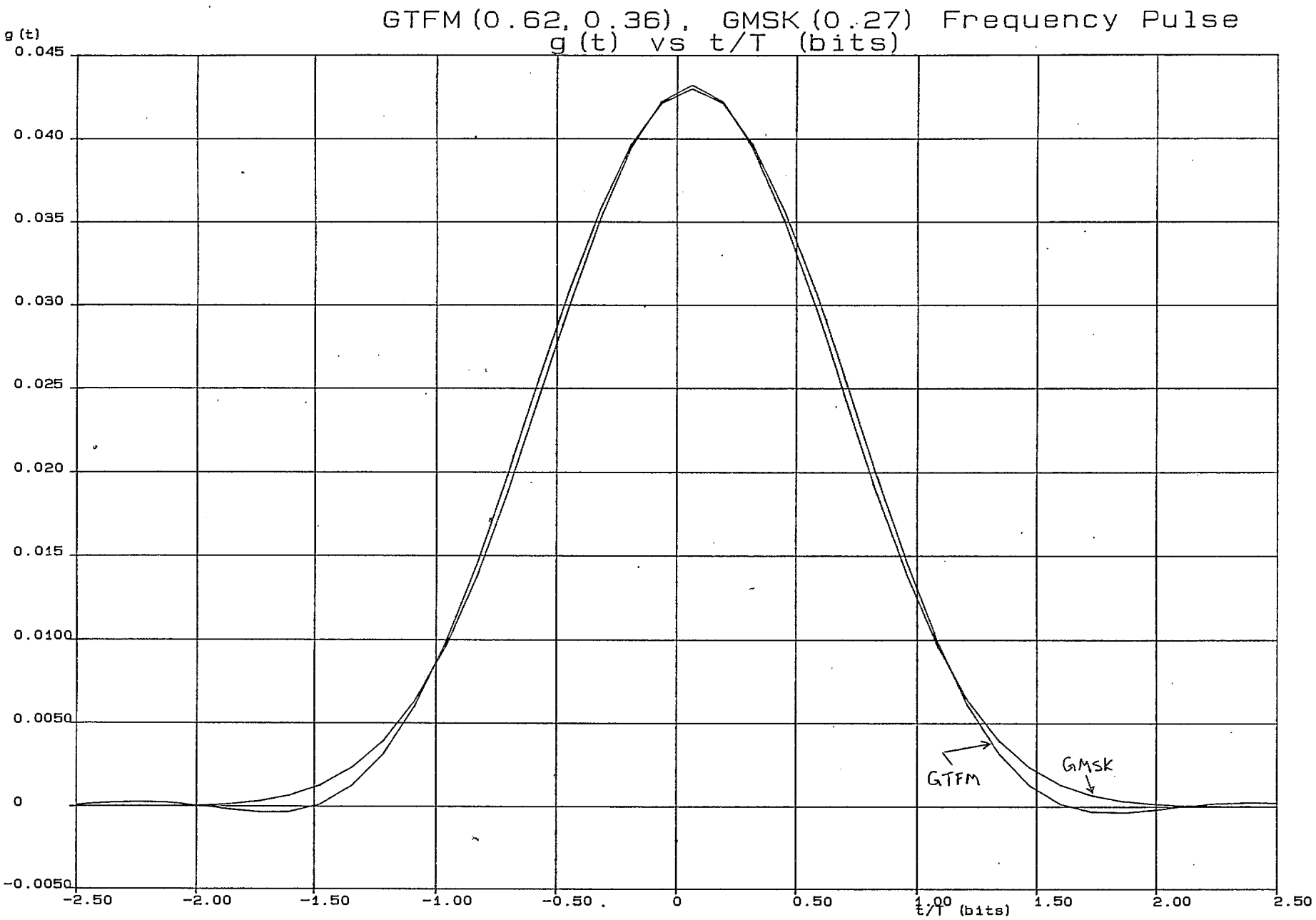
GTFM (0.62, 0.36), GMSK (0.27) Frequency Pulse
g(t) vs t/T (bits)
g(t)
0.045
0.040
0.035
0.030
0.025
0.020
0.015
0.0100
0.0050
0
-0.0050
-2.50
-2.00
-1.50
-1.00
-0.50
0
0.50
1.00
1.50
2.00
2.50
t/T (bits)
GTFM
GMSK

Figure 2.3.7

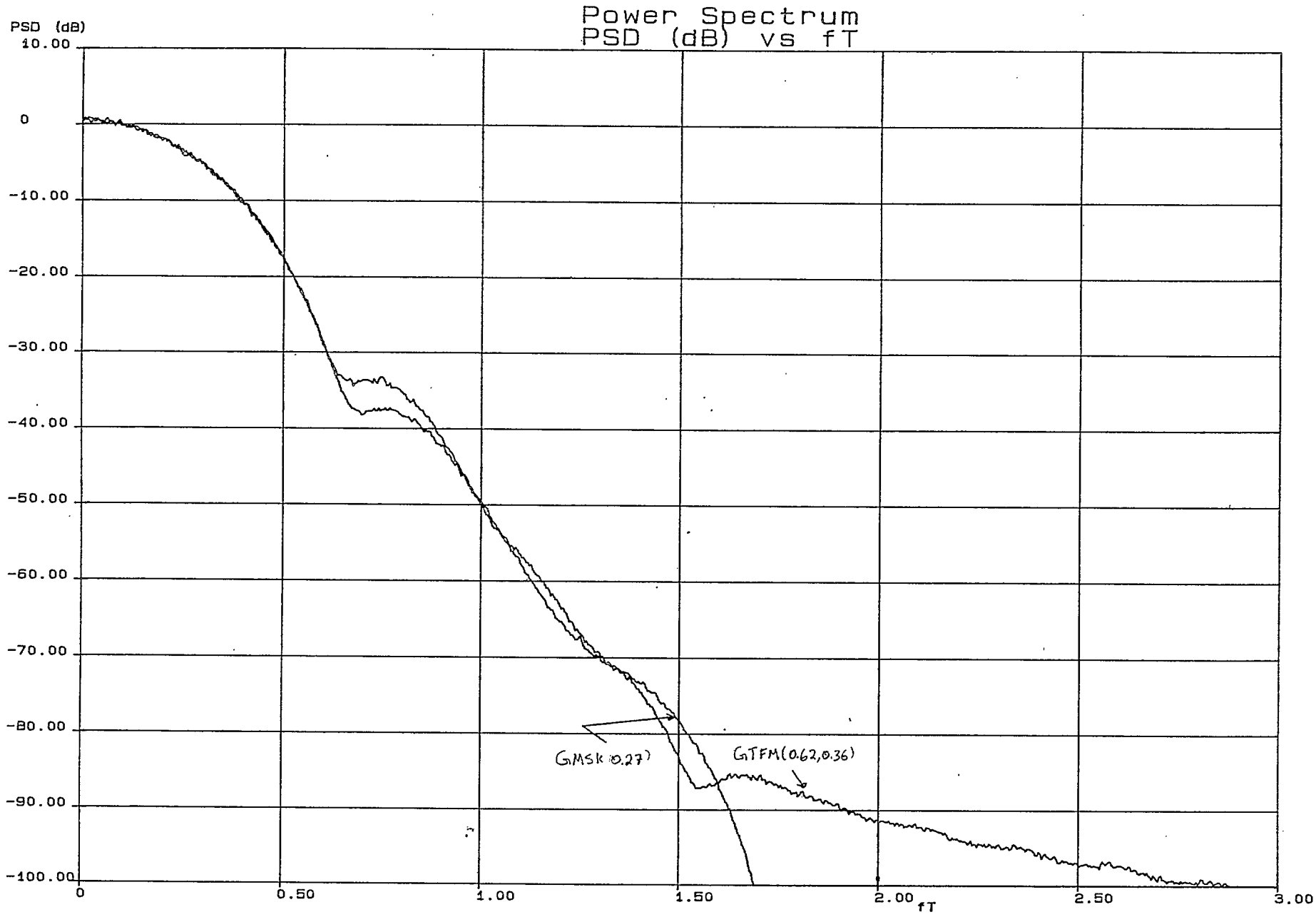
Power Spectrum
PSD (dB) vs fT
PSD (dB)
10.00
0
-10.00
-20.00
-30.00
-40.00
-50.00
-60.00
-70.00
-80.00
-90.00
-100.00
0
0.50
1.00
1.50
2.00
2.50
3.00
fT
GMSK 0.27)
GTFM(0.62,0.36)

Figure 2.3.8

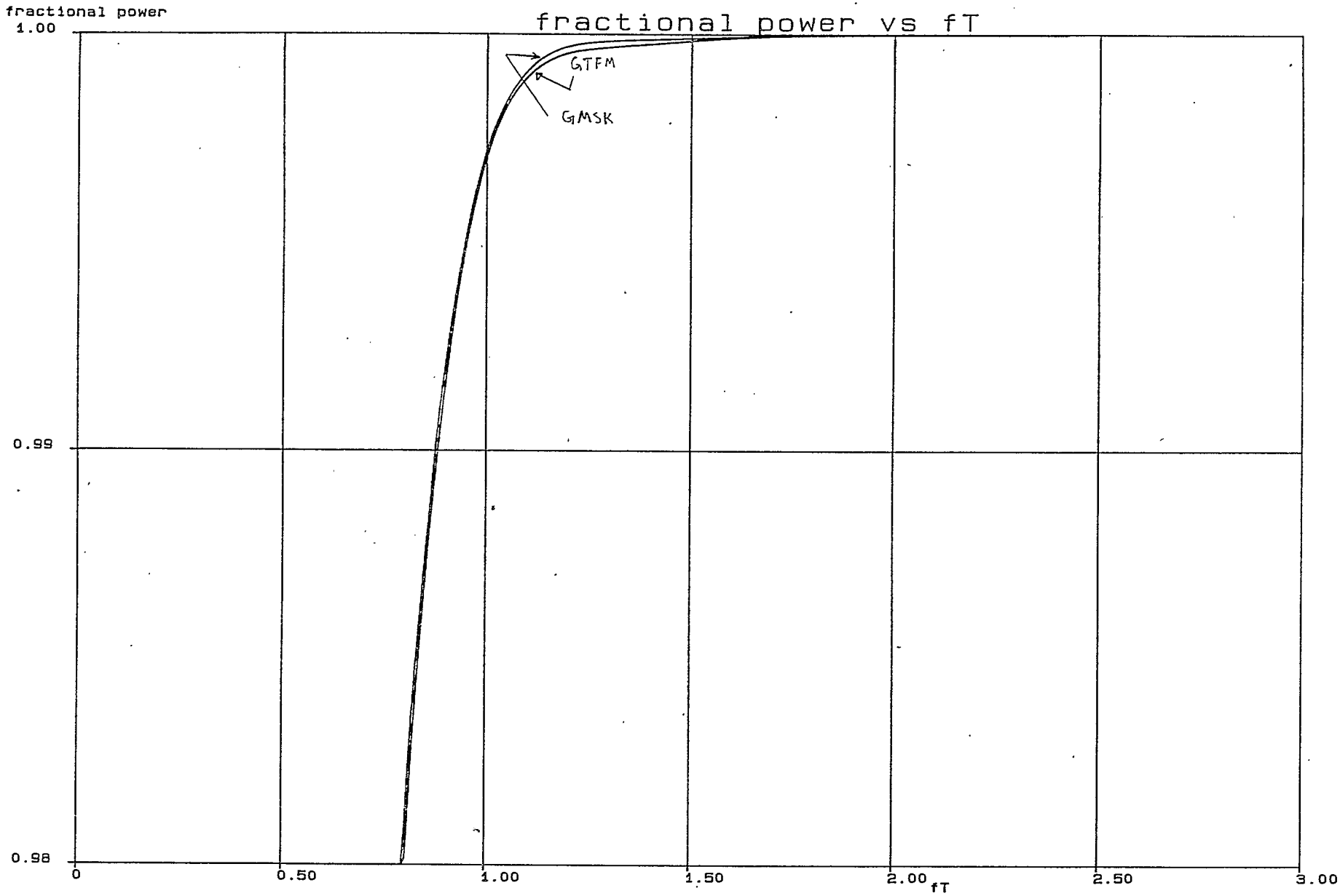
fractional power
fractional power vs fT
1.00
0.99
0.98
GTFM
GMSK
0
0.50
1.00
1.50
2.00
2.50
3.00
fT

Figure 2.3.9

2.4 Channel Model

The physical model of the communications link at a block diagram level and the underlying model (figure 2.4.1) can be represented mathematically as:

$$r(t) = g(t)v(t,\underline{\alpha}) + n(t)$$

The additive noise n(t) is a complex random process with gaussian pdf having real and imaginary components with two sided power spectral density N_o watts/Hz [21].

Due to multipath propagation the signal at the (assumed moving) receiver is subject to constructive and destructive interference. With enough scattered field components, we may invoke the central limit theorem and claim that:

$$g(t) = L + g_r(t)$$

where L is the line of sight component and $g_r(t)$ is a zero mean complex gaussian process.

The amplitude distribution can be modeled as a complex gain g(t) having uniform random phase in $[-\pi,\pi]$ and amplitude distribution obeying a Rician pdf.

The amplitude distribution of the received envelope degrades to a Rayleigh distribution as the line of sight component diminishes. The Rayleigh channel is characterized by quasi-periodic fades (often > 40 dB), and corresponding rapid phase fluctuations. The frequency of the fades is proportional to the doppler frequency f_D where:

$$f_D = f_c v/c$$

where v = the vehicle speed,

c = speed of light,

f_c = carrier frequency.

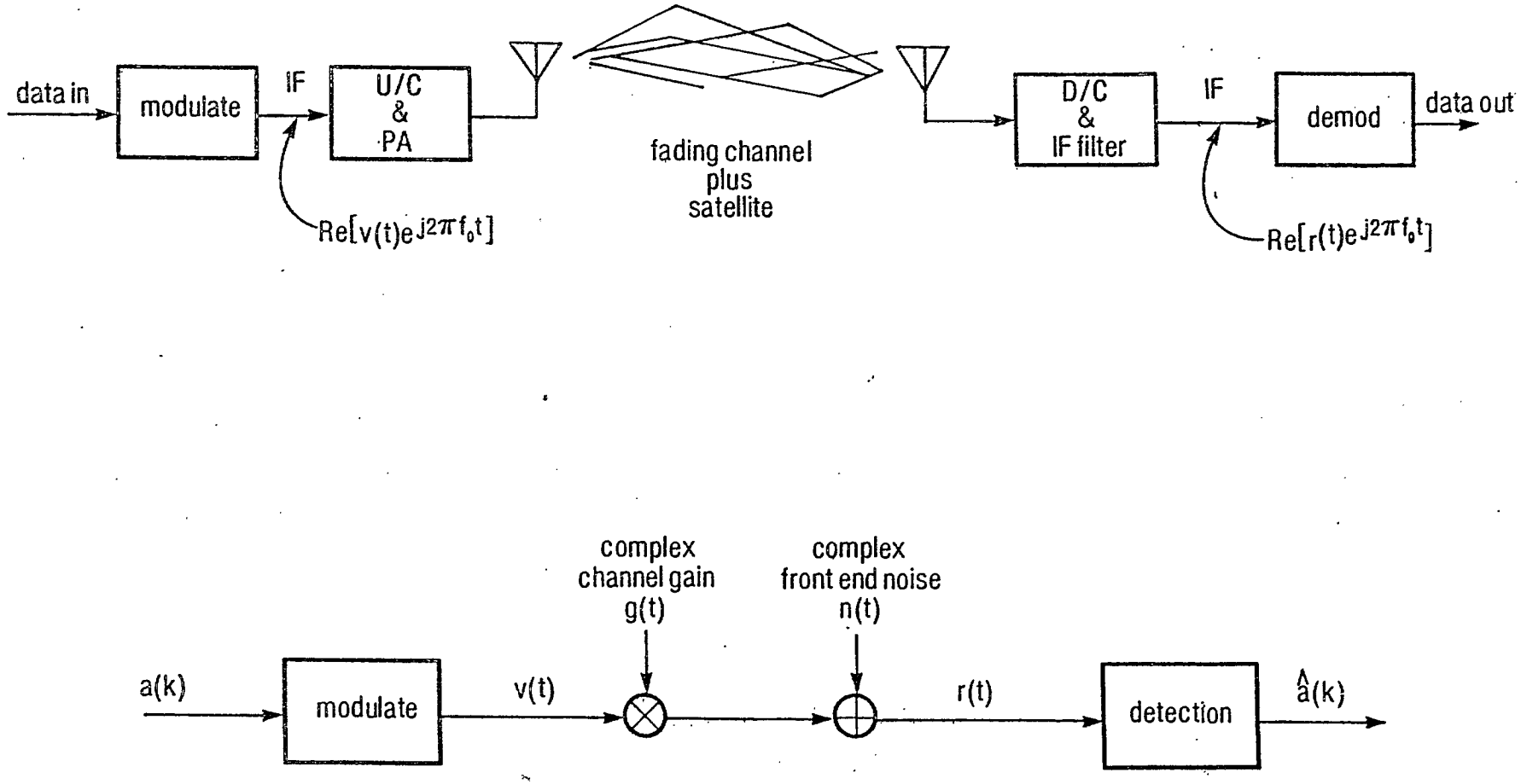
data in
modulate
IF
U/C
&
PA
Re[v(t)e^{j2πf_0t}]
fading channel
plus
satellite
D/C
&
IF filter
IF
demod
data out
Re[r(t)e^{j2πf_0t}]
a(k)
modulate
v(t)
complex
channel gain
g(t)
complex
front end noise
n(t)
r(t)
detection
â(k)

Figure 2.4.1

Rapid phase fluctuations have a detrimental effect on both coherent and incoherent receivers. Both receivers work poorly since the rapid phase fluctuations due to the channel can be on the same order of magnitude as the phase changes due to the data, hence the term random frequency modulation (or random FM). Even in the noise free case, this random FM may cause errors. Thus, the receiver has an irreducible error rate, (and, of course, increasing transmitter power will not help). The only solution is to increase the data rate, although this is not always desirable, due to bandwidth and power constraints. Coherent receivers are often inferior to incoherent receivers due to the rapidly changing phase which is difficult, if not impossible, to be track accurately.

Typical BER curves in the fading environment are shown in figure 2.4.2. This short introduction to the problem of communications in a fading environment is by no means complete. Specification of RF spectra of the received field components and power spectra of random FM is dealt with in detail in [22].

Our simulations assume $g(t) = 1$, (a static channel). Although inferences can be made from these results on the performance of the receiver in a amplitude fading environment (no random FM), the irreducible error rate due to random FM is unknown.

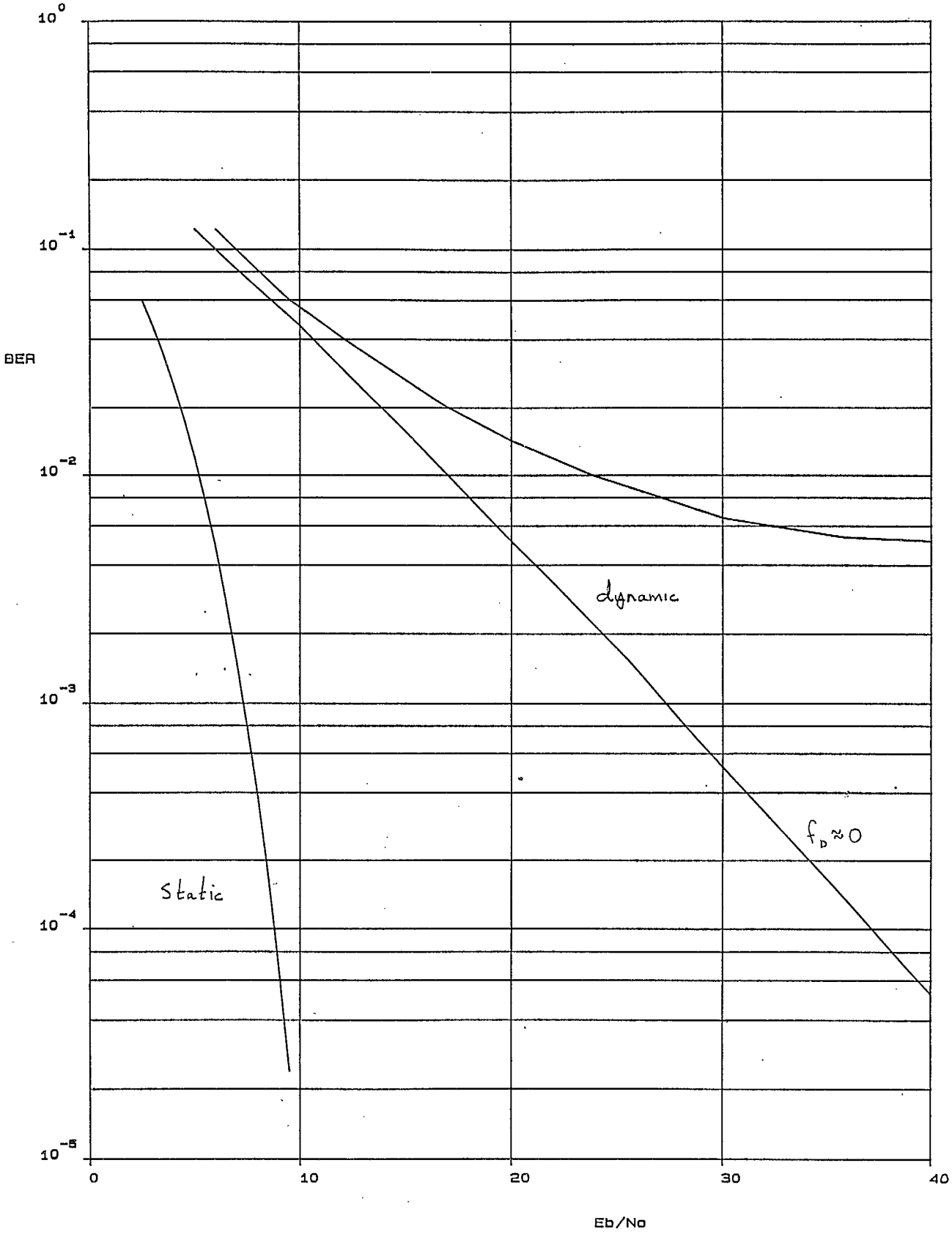
10^{0}
10^{-1}
10^{-2}
10^{-3}
10^{-4}
10^{-5}
BER
0
10
20
30
40
Eb/No
Static
dynamic
$f_D \approx 0$

Figure 2.4.2

2.5 Modem Interfaces and Major States

The modem has the functional organization shown in figure 2.5.1. The DTE communicates to the modem (DCE) over a synchronous RS232 interface subset. The modem has a 4800 Hz IF interface.

The modem is to operate in full duplex fashion and synchronize itself in both time (bit clock) and frequency upon an initial preamble. The modem will be able to handle up to a +/- 400 Hz offset in the received signals center frequency.

The data rate is 4.8 kbps, nominal channel centers are to be spaced 5 kHz apart and adjacent channels can be up to 13 dB higher than the desired channel when received by the base station.

The major states of the modem can be pictured as in figure 2.5.2. When not actively receiving data, the modem sits in a synch hunt state, continuously trying to acquire carrier frequency and bit clock. When a signal of sufficient strength and correct format appears, the modem locks on, and enters the demod state. In this state it demodulates the incoming signal, tracks bit timing and delivers the data to the DTE by means of RD and RC. If the signal strength falls below a threshold for more than the hangover time T_h, the modem considers the transmission to be finished, and returns to the synch hunt state. The hangover interval lets the modem bridge short fades, but introduces a latency period before it can receive or transmit again, thereby increasing the effective duration and traffic load of the transmission.

An alternative sequence takes place if the DTE decides to transmit by asserting RTS. The modem then keys the transmitter, transmits the preamble and supplies bit clock while transmitting data. When the DTE negates RTS, the modem stops transmitting, and returns to the synch hunt mode.

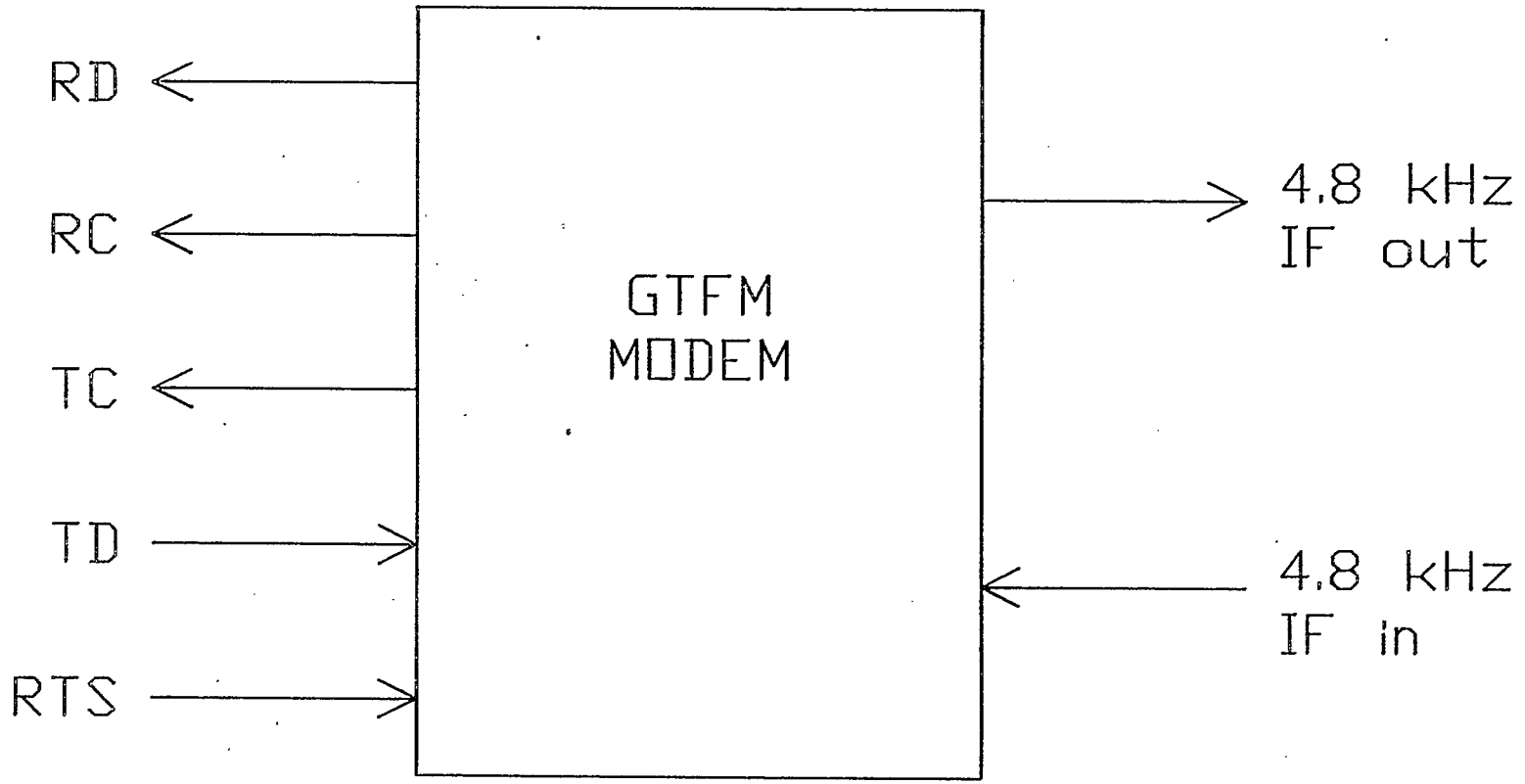

Figure 2.5.1

Modulation States

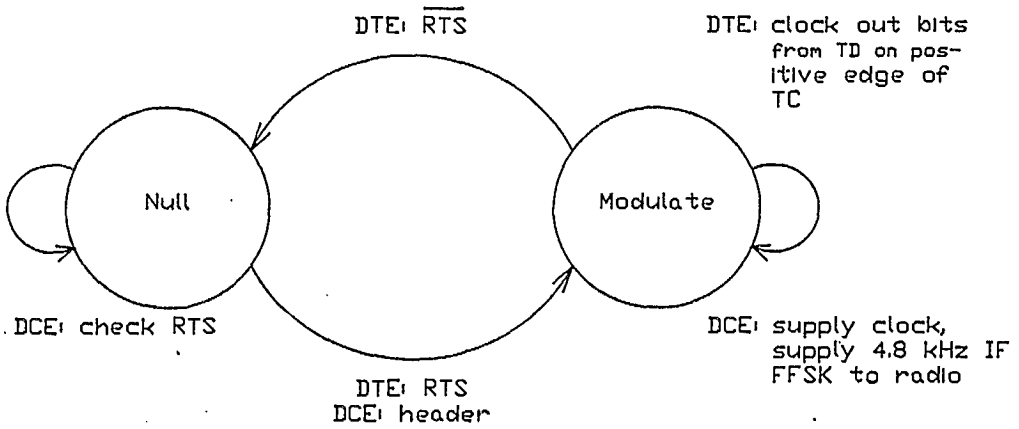

Demodulation States

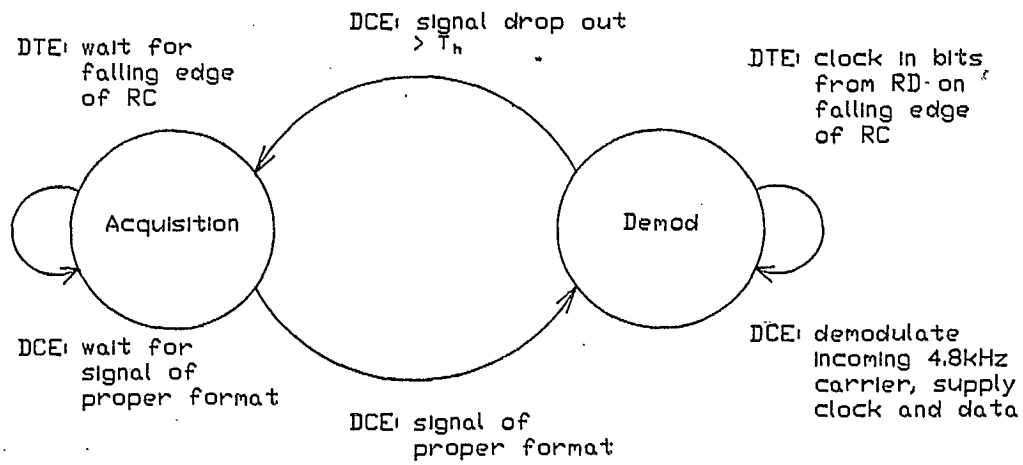

Figure 2.5.2

3. DEMODULATION

In this section we review the two general classes of demodulators for CPM, coherent and incoherent.

3.1 Coherent Demodulation

As discussed in section 2.5 the channel is assumed to add zero mean, white gaussian distributed noise with two sided noise power spectral density N_o watts/Hz. Thus we receive:

$$r(t) = v(t,\underline{\alpha}) + n(t) \qquad -\infty \leq t \leq \infty$$

The optimum coherent detector, (which is the optimum detector), in terms of minimizing the probability of error over a sequence of bits chooses that sequence of bits, $\hat{\underline{\alpha}}$ for which $v(t,\hat{\underline{\alpha}})$ is closest (in a mean square sense) to r(t). Or, to paraphrase [1], the detector which minimizes the probability of error chooses the sequence $\hat{\underline{\alpha}}$ which minimizes the probability of error.

The optimum detector maximizes the log likelihood function[21]:

$$\log(\Omega'_N[r(t)]) = \int_{-\infty}^{\infty} r(t)v(t,\hat{\underline{\alpha}})dt$$

With an infinite number of sequences possible this method does not seem tractible. However, a recursive algorithm, known as the Viterbi algorithm (VA, a maximum likelihood sequence estimator, MLSE) originally intended for decoding convolutional codes [16] is applicable in this instance [17,18]. In this case, h must be a rational number, (although it should be rational, anyway, for coherent phase tracking). The complexity (the number of states) increases geometrically depending on the number of bits over which the (controlled) intersymbol interference extends (L), and h the modulation index. The modulation index h = p/q, where p is relatively prime to q.

With these definitions, the number of states is just:

$$2 \cdot q \cdot 2^{L-1}$$

For example, for GTFM(0.62,0.36), h = 1/2 (p=1, q=2), and L = 3, the

number of states is just:

$$2 \cdot 2 \cdot 2^{3-1} = 16$$

Sub-optimum detectors, described in the literature [1,2,4], often perform the correlations over a finite number of bits, and base the decision on this information.

Optimum demodulation of differentially encoded MSK may proceed by maximizing the likelihood function. However, this function is also maximized using the popular quadrature coherent demodulator [3].

GMSK and GTFM may also use this structure to obtain near optimal decisions on received symbols [5,6,7,10].

3.2 Optimum Incoherent Detection

Optimum incoherent detection of CPM, (optimum in terms of minimizing the probability of error in detecting a single bit) formulated in [4], although applied to CPFSK (which belongs to the class of full response CPM), is applicable here.

The optimum detector maximizes z^+ and z^- where:

$$z^+ = \sum_n I_o(2/N_o\ (r(t),v(t,\underline{\hat{\alpha}}_n^+)))$$

where

$\underline{\hat{\alpha}}_n^+$ is the n^{th} sequence with a +1 in the middle bit ($\hat{\alpha}_k$),

and

$(r(t),v(t,\underline{\hat{\alpha}}_n^+))$ is the inner product of $r(t)$ with $v(t,\underline{\hat{\alpha}}_n^+))$

(i.e. $(r(t),v(t,\underline{\hat{\alpha}}_n^+)) = \int_{-\infty}^{\infty} r(t)v(t,\underline{\hat{\alpha}}_n^+)dt$),

and where:

$$z^- = \sum_n I_o(2/N_o\ (r(t),v(t,\underline{\hat{\alpha}}_n^-)))$$

where

$\underline{\hat{\alpha}}_n^-$ is the n^{th} sequence with a -1 in the middle bit ($\hat{\alpha}_k$).

The optimum detector chooses $\hat{\alpha}_k = +1$ if $z^+ > z^-$ and $\hat{\alpha}_k = -1$ otherwise. In order to minimize computation (somewhat), the sub-optimum detector correlates over a window of W bits, and the maximum value of the correlation determines the middle bit. The approximations involved are discussed in detail in [4,23] to yield the detector which maximizes:

$$s^+ = \max_n \int_{-W/2}^{W/2} r(t)v(t,\underline{\hat{\alpha}}_n^+)dt$$

$$s^- = \max_n \int_{-W/2}^{W/2} r(t)v(t,\underline{\hat{\alpha}}_n^-)dt$$

The middle bit, $\hat{\alpha}_k$, is chosen to be +1 if $s^+ > s^-$, -1 otherwise.

3.3 Differential Detection

The differential detector computes the differential phase over one bit period in order to make a decision on the received bit.

We have:

$$r(t) = v(t,\underline{\alpha}) + n(t) \qquad -\infty \leq t \leq \infty$$

The received signal is first filtered to attenuate out of band noise and adjacent channels.

Thus, the signal prior to differential detection is:

$$r'(t) = r(t) * h(t)$$

where

* denotes convolution,

h(t) is the convolved impulse response of the front end filter and channel.

The differential detector computes the differential phase:

$$y_k = \text{Arg}(r'(t)(r'(t-T))^*)$$

where

$(\cdot)^*$ denotes complex conjugation,

and $\text{Arg}(\cdot)$ is the principal value of the argument, defined in $[-\pi,\pi]$.

Although the distortion in the phase of r(t) due to the front end filter is non-linear, we approximate the distortion with a linear model. We define, $\underline{f}$ as the sampled impulse response of the modulator, channel, and front end filter.

For any CPM scheme in which the composite impulse response extends (to a good approximation) over L bits, we can approximate the differential phase over one bit as:

$$\hat{\phi}(k,\underline{\alpha}) = \underline{f} * \underline{\alpha}_k$$

where

* denotes convolution

$\underline{\alpha}_k = \alpha_{k-L+1}, \alpha_{k-L+2}, \ldots, \alpha_k$

and

$\underline{f} = f_0, f_1, \ldots, f_{L-1}$

$\underline{f}$ is the sampled composite impulse response of the channel.

Thus:

$$\hat{\phi}(k,\underline{\alpha}) = f_0\alpha_k + f_1\alpha_{k-1} + \ldots + f_{L-1}\alpha_{k-L+1}$$

Again, recall that this is just an approximation, since impulse response; and convolution only make sense with linear systems. However, continuing with our linear model we have:

$$y_k = f*\phi(k,\underline{\alpha})+n_k$$

To unravel the intersymbol interference terms we may use a maximum likelihood sequence estimator (MLSE).

If y_k were corrupted by additive white gaussian noise the maximum likelihood sequence estimator chooses that sequence (as the best sequence) which maximizes:

$$\sum(y_k - \hat{\phi}(k,\underline{\hat{\alpha}}))^2$$

Although the noise, n_k, is neither white, nor gaussian, nor independent of the signal, the above estimator is still useful, and a better estimator may be difficult to find. Thus, we choose the MLSE for lack of a better estimator.

Although straightforward calculation of the above summations is out of the question, a recursive scheme, (the Viterbi algorithm) allows us to maximize this equation sequentially. The complexity doubles for every unit increase in L, so only small values of L are useful.

Two values of L are to be investigated, L = 2, and L = 3. In section 4.3 it is shown that these approximations are valid.

For L = 2, and a symmetric impulse response, the differential phase

obeys the duo-binary rule.

Thus:

$$\hat{\phi}(k,\underline{\hat{\alpha}}) = 1/2\ (\hat{\alpha}_{k-1} + \hat{\alpha}_k)$$

Bit by bit detection on y_k can be performed by first differentially encoding the data:

$$b_k = \hat{\alpha}_k b_{k-1}$$

$$\hat{\phi}(k,\underline{\hat{\alpha}}) = \pi h/2(b_{k-1} + b_k)$$

$$= \pi h/2\ b_{k-1}(1 + \hat{\alpha}_k)$$

Thus, with $h = 1/2$:

$$\hat{\alpha}_k = +1 \text{ if } |y_k| > \pi/4$$

$$\hat{\alpha}_k = -1 \text{ if } |y_k| < \pi/4$$

The bit by bit detector is shown in figure 3.3.1. The bit by bit differential detector computes:

$$w_k = \mathrm{Re}[r'(t+kT)r'^{*}(t+(k-1)T)]$$

$$= \mathrm{Re}[\exp(j\hat{\phi}(k,\underline{\hat{\alpha}})-\hat{\phi}(k-1,\underline{\hat{\alpha}})) + \exp(j\hat{\phi}(k,\underline{\hat{\alpha}}))n_{k-1} + \exp(j\hat{\phi}(k-1,\underline{\hat{\alpha}}))n_k + n_k n_{k-1}]$$

$$= \cos(\hat{\phi}(k,\underline{\hat{\alpha}})-\hat{\phi}(k-1,\underline{\hat{\alpha}})) + \text{noise terms}$$

The decision regions for the differential phase are:

$$\hat{\alpha}_k = +1 \text{ for } |\hat{\phi}(k,\underline{\hat{\alpha}})-\hat{\phi}(k-1,\underline{\hat{\alpha}})| > \pi/4$$

$$\hat{\alpha}_k = -1 \text{ for } |\hat{\phi}(k,\underline{\hat{\alpha}})-\hat{\phi}(k-1,\underline{\hat{\alpha}})| < \pi/4$$

Thus, the slicing levels after the $\cos(\cdot)$ non-linearity should be set at $\cos(\pi/4) = 1/\sqrt{2}$.

Although bit by bit detection works, the performance with respect to a maximum likelihood sequence estimator is quite poor. Recall, for $L = 2$, the received differential phase obeys the duo-binary rule:

$$\hat{\phi}(k,\underline{\hat{\alpha}}) = 1/2\ (\hat{\alpha}_{k-1} + \hat{\alpha}_k)$$

and for $L = 3$,

$$\hat{\phi}(k,\underline{\hat{\alpha}}) = f_2\hat{\alpha}_{k-2} + f_1\hat{\alpha}_{k-1} + f_0\hat{\alpha}_k$$

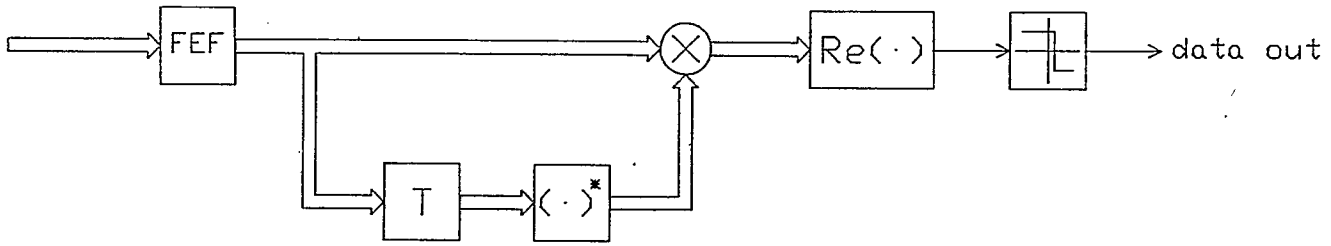

Figure 3.3.1

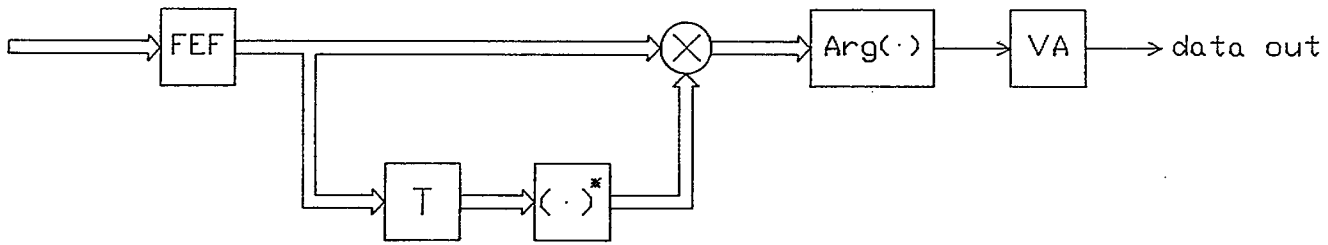

Figure 3.3.2

The maximum likelihood sequence estimator maximizes:

$$\sum_{k=-\infty}^{\infty}(y_k - \hat{\phi}(k,\hat{\underline{\alpha}}))^2$$

A recursive solution for maximizing this summation is given in Appendix A, and references [17,18,19,20].

Differential encoding of the data is also advisable when the four state (L=3) MLSE is used, see [19].

The differential detector based on maximum likelihood sequence estimation is shown in figure 3.3.2.

The one bit period delay used in the differential detector is not claimed to be optimum, (although it is for MSK). The Japanese claim a two bit differential detector is superior for GMSK, (see section 3.5), although increasing the time delay only increases the amount of intersymbol interference. It should also be noted that when the delay becomes very small, the differential phase approaches a crude derivative of the phase, and hence the differential detector approaches a discriminator.

3.4 Discriminator Detection

The discriminator computes the derivative of the received phase function in order to make decisions on received data symbols. As discussed in section 3.3 we receive (after front end filtering, and hard limiting):

$$r'(t) = r(t)*h(t)/|r(t)*h(t)|$$
$$= \exp(j\theta(t))$$

We require:

$$y(t) = d\theta(t)/dt$$

We compute:

$$y(t) = \mathrm{Im}[(dr'(t)/dt)^{*}r'(t)]$$
$$= \mathrm{Im}[jd\theta(t)/dt\ \exp(j\theta(t))\exp(-j\theta(t))]$$
$$= d\theta(t)/dt$$

The sampled outputs are y_k.

We define $\underline{f}$ as the sampled impulse response of the modulator, channel, front end filter and discriminator. (Note that in the absence of channel and front end filter that the impulse response is equal to the frequency pulse g(t)). Again the distortion due to the front end filter is non-linear, but we assume we can approximate the distortion with a linear model.

For any CPM scheme in which the composite impulse response extends (to a good approximation) over L bits, we can approximate the received (sampled) derivative of the phase as:

$$y_k = d\hat{\phi}(k,\underline{\alpha})/dt + n_k$$
$$= \underline{f}*\underline{\alpha} + n_k$$

This is the same relation obtained for differential detection of CPM, although $\underline{f}$ is not equivalent to that obtained for differential detection, and the noise n_k has different properties. Thus, we can use a bit by bit detector, or a MLSE of (hopefully) modest complexity to unwind the

intersymbol interference. The discriminator detector is shown in figure 3.4.1. As with differential detection, differential encoding prior to modulating the data, and differential decoding on reception is advisable.

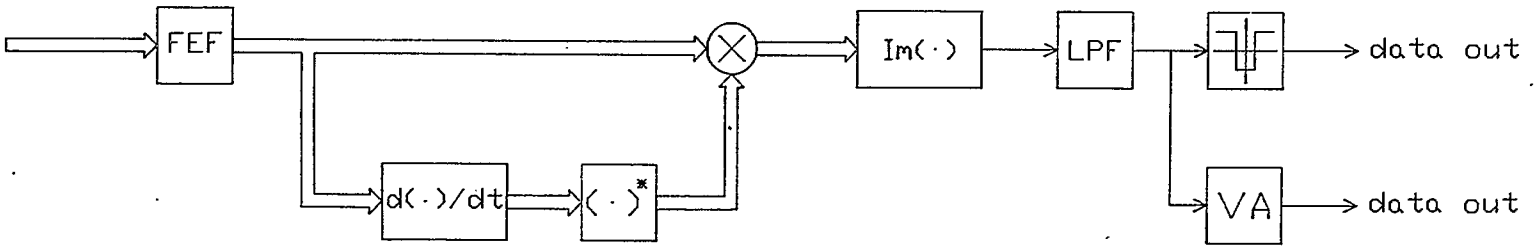

Figure 3.4.1

3.5 Performance Obtained in the Literature

Static performance for coherent detection of GMSK or GTFM using MSK type coherent receivers is presented in numerous papers [5,6,7,10].

Degradation of TFM (GTFM(0.50,0.0)), [5,6], from ideal coherent detection of differentially encoded MSK (coherent fast FSK, CFFSK) is approximately 1.0 dB at an error rate of 10^{-2}. Similar performance is obtained for coherent detection of GMSK(0.25). GTFM(0.62,0.36) performance is superior with a degradation of only 0.30 dB from coherent FFSK (again at a BER of 10^{-2}). The power spectrum and coherent BER performance (static) for GTFM with various B,r combinations, and GMSK with various BT products is shown in figures 3.5.1 to 3.5.4, from [6,10]. From these figures it appears that GTFM(0.62,0.36) is near optimum in terms of maintaining a compact power spectrum while maintaining good coherent BER performance.

The poor performance of TFM with coherent detection in a Rayleigh fading environment is demonstrated in [7,8]. The irreducible BER is more than two orders of magnitude poorer for coherent detection, than for incoherent (discriminator) detection (see figure 3.5.5, 3.5.6). At 40 Hz doppler the irreducible bit error rate for coherent detection is $> 10^{-2}$ and $\approx 10^{-4}$ for noncoherent detection, (discriminator), figure 3.5.9.

Mobile field experiments in the Tokoyo and Yokosuka areas [11] discovered a factor of ten difference between the irreducible BER of coherent detection with respect to incoherent detection (differential, cos(T)) at a 40 Hz doppler frequency (figure 3.5.7).

Since both papers are assuming transmission at 16 kbps we may infer that the coherent detector used in [11] offered an improvement of a factor of ten over the performance in [8] (in terms of irreducible error rate) and that discriminator detection performs as well or slightly better than a differential detector in the presence of random FM. This statement is

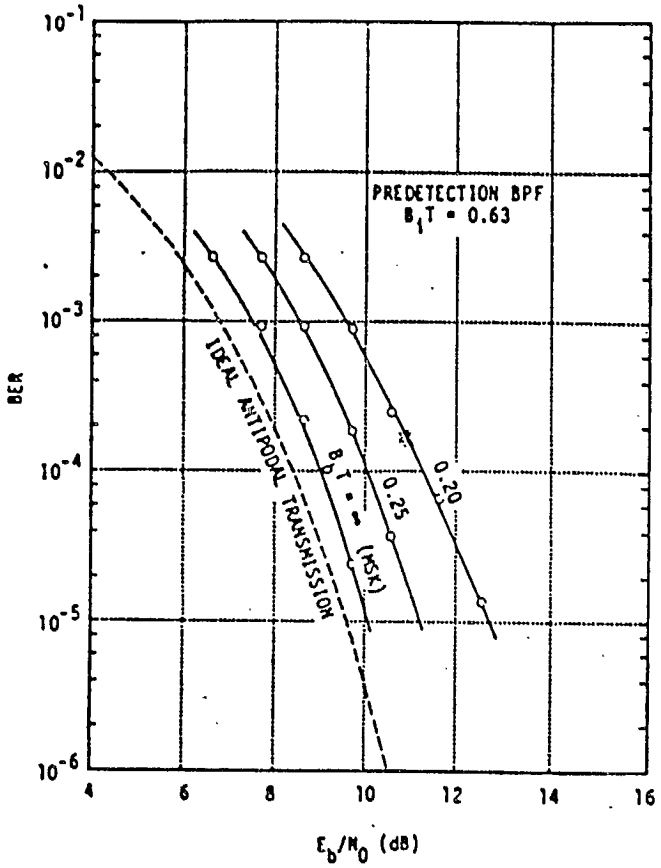

Figure 3.5.1

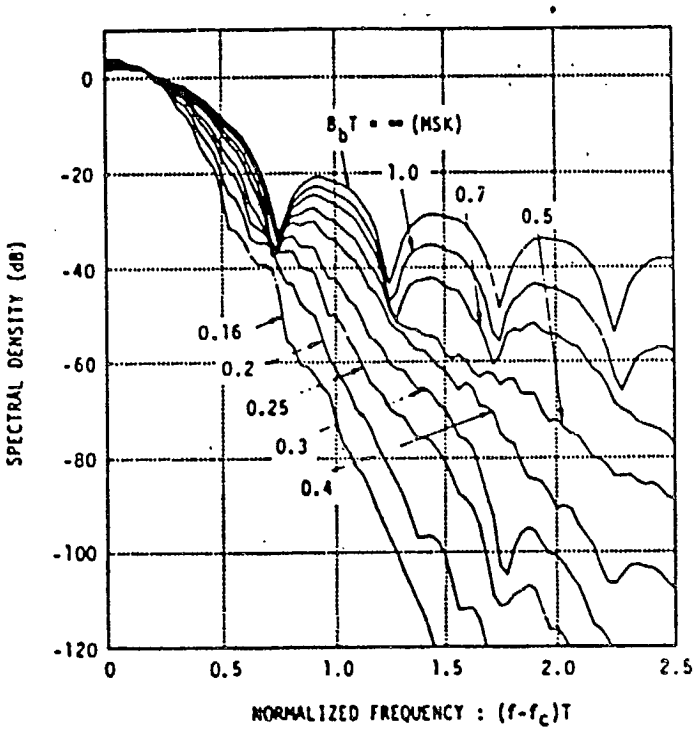

Figure 3.5.2

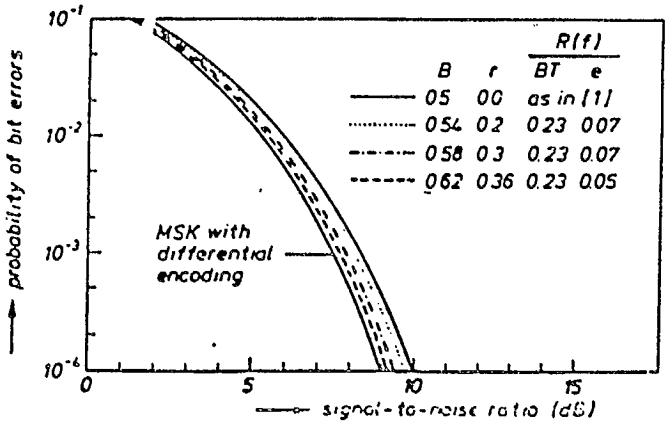

Figure 3.5.3

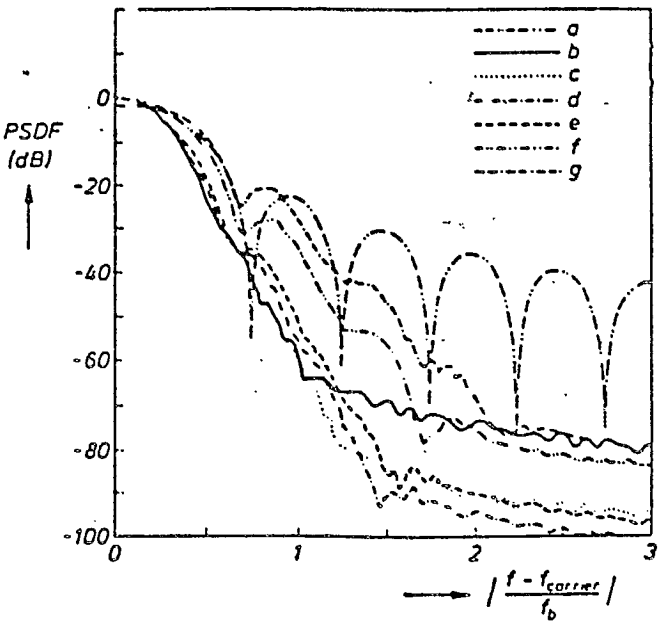

Figure 3.5.4

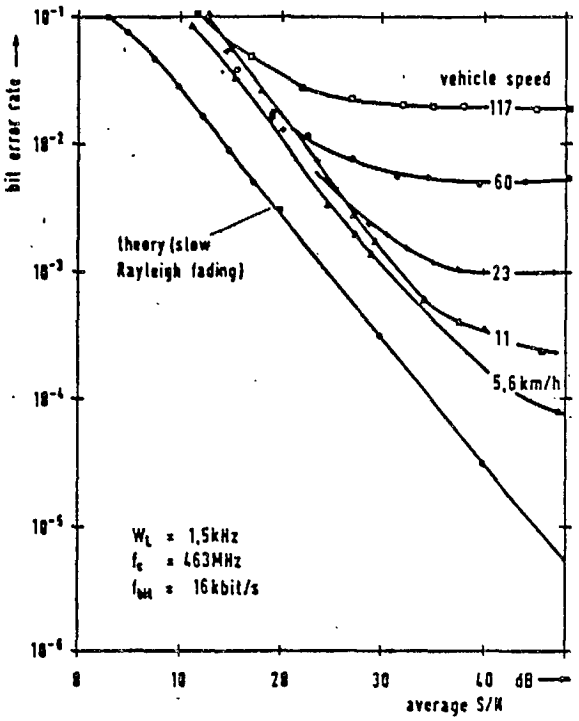

Figure 3.5.5.

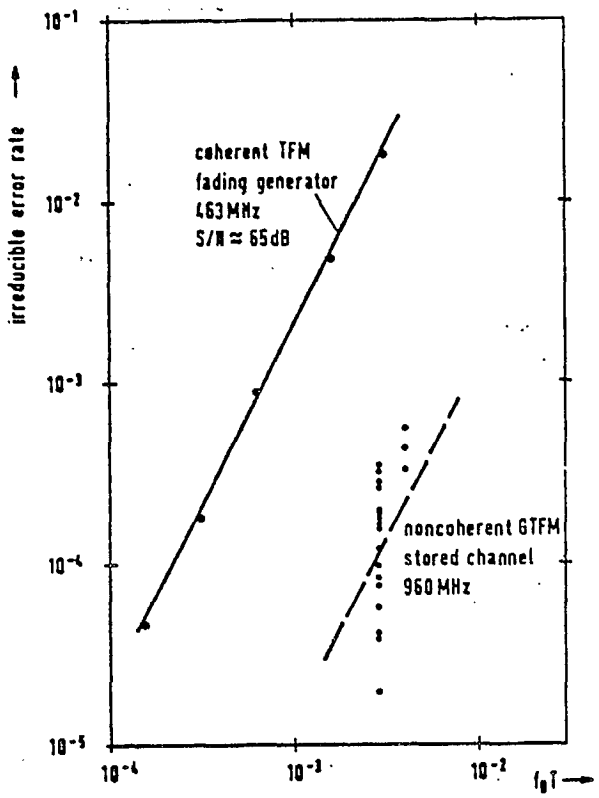

Figure 3.5.6

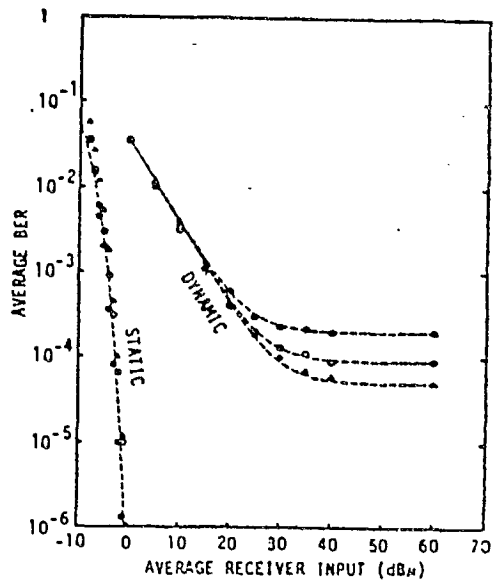

Figure 3.5.7

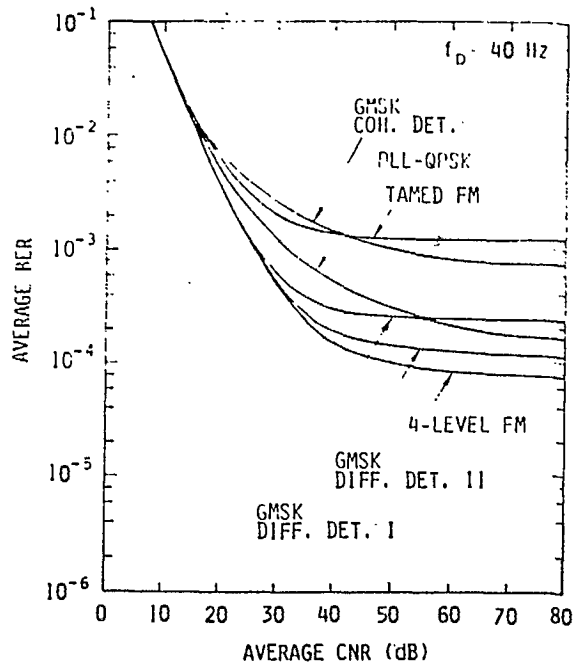

Figure 3.5.8

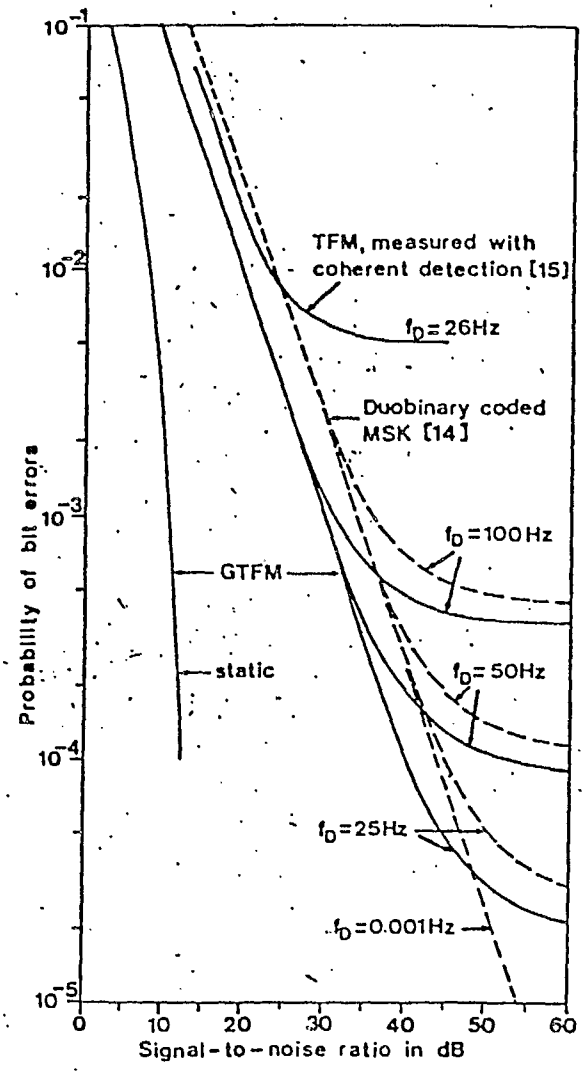

Figure 3.5.9

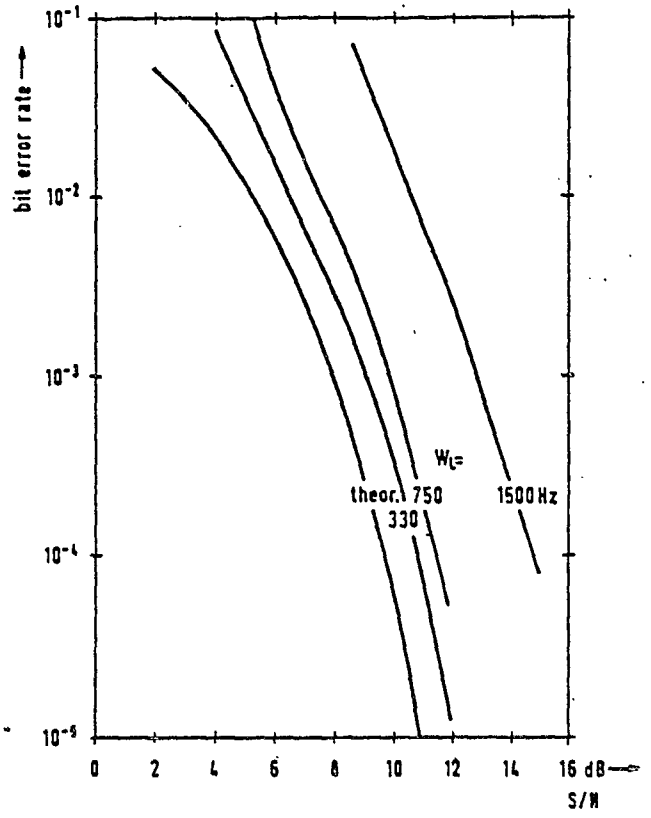

Figure 3.5.10

supported by [12] in which both GMSK(0.25) and TFM with coherent detection were studied. The results showed an order of magnitude improvement in the irreducible error rate over [8], (for TFM, 40 Hz doppler, figure 3.5.8). The static performance of the coherent detector used in [8] degrades rapidly as the bandwidth of the Costas loop increases. In fact, a loss of more than 4 dB in the static performance of the demodulator in [8] was incurred in increasing the noise bandwidth of the Costas loop, (figure 3.5.10). The static performance in [12] is not comparable to that in [8] due to different signal to noise ratio measurements used.

To make matters worse, at 4.8 kbps the random FM effect will be worse (for equivalent f_d) than at 16 kbps. With these points in mind, we hope incoherent detection will provide us with better performance.

The performance of optimum incoherent detection of TFM [13] (figure 3.5.11), optimized discriminator detection of GTFM(0.62,0.36) [6] (figure 3.5.12), and optimized differential detection of GMSK(0.25) [12] (figure 3.5.13) offer close to equivalent performances, ($\approx 10^{-2}$ at E_b/N_o = 8 dB). Whether the above comparisons are valid, since different modulation methods are used, is an important question. GMSK(0.25) and GTFM(0.62,0.36) are approximately equal in terms of radiated power spectrum, but TFM has a somewhat more compact power spectrum.

As is evident [12] (figure 3.5.12) either uses their own measure of signal to noise ratio and not E_b/N_o or their coherent GMSK curve is one dB poorer than that obtained in [10]. To make matters worse, [12] claims coherent GMSK(0.25) is 2 dB better than coherent TFM at a BER of 10^{-2}. Either their TFM curve is just plain incorrect, or they have found a coherent detector for GMSK(0.25) which performs 1 dB better than optimum coherent FFSK, (since TFM is only 1 dB poorer than CFFSK). One would expect they have not found a demodulator which performs better than the

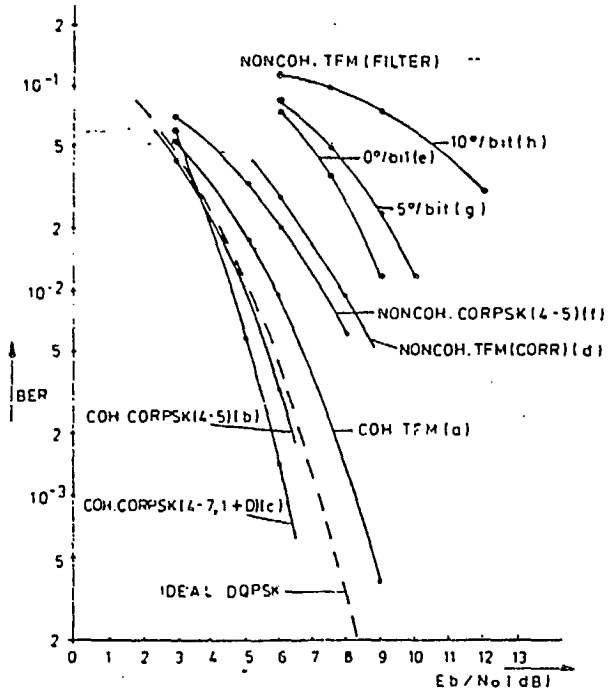

Figure 3.5.11

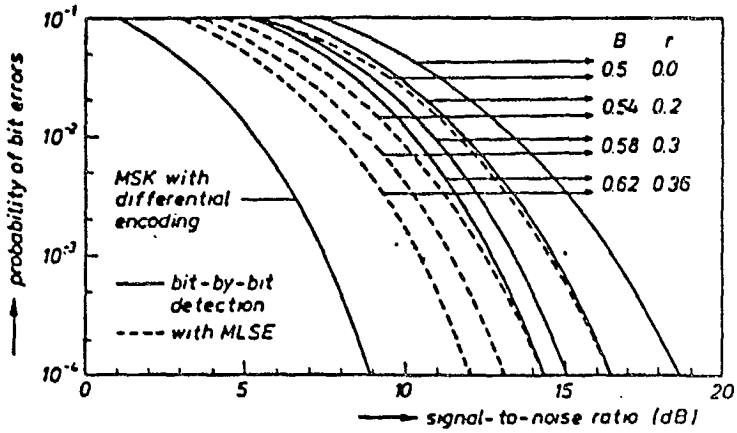

Figure 3.5.12

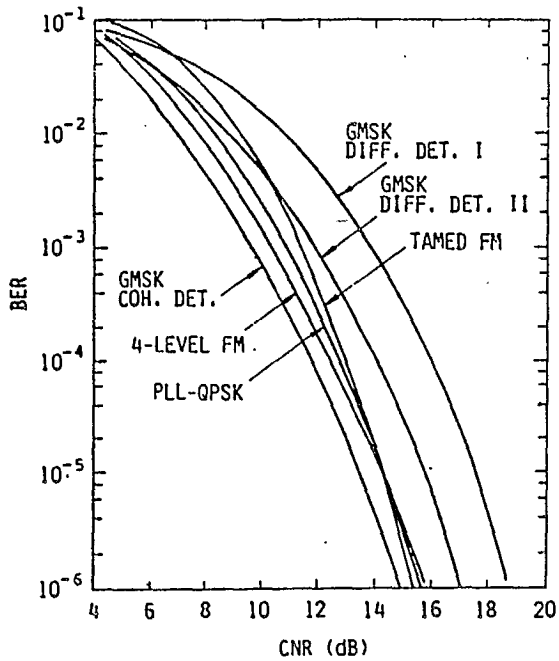

Figure 3.5.13

optimum. (Sometimes one must wonder what exactly the Japanese are doing, and in fact if they themselves know). In any event, we take as our reference (for this curve) coherent GMSK(0.25) and hope it is the same as that found in other papers such as [10].

Returning to optimum incoherent detection for a moment, the window length used in [13] was eight bits long, making the computation somewhat unfeasible. The window length for GTFM(0.62,0.36) might be shortened, (since the frequency pulse is somewhat narrower than for TFM), and the performance gain might be a fraction of a dB. However, using a window length of seven bits and decision feedback, we would still need to compute 2^4 complex correlations, each seven bits long. Using four samples per bit, this would require:

$$16 \cdot 28 = 448 \text{ complex multiply/adds}$$

$$= 1792 \text{ real multiply/adds}$$

Although more simplifications exist, the complexity involved does not seem to warrant further investigation in order to save a fraction of a dB.

3.6 Summary

In this section we have studied various detectors from a theoretical standpoint, and the performance obtained in the literature.

However, now that total confusion has set in after comparing results over a seemingly endless number of papers, almost all using their own definition of signal to noise ratio, half the results due to simulation and the other half experimental results, the task of choosing an acceptable demodulation technique must be accomplished.

The performance of differential detectors and discriminators appears to be quite similar, albeit a little unknown for similar modulation techniques, and in general, coherent receivers provide poor performance due to random FM effects. A simple maximum likelihood sequence estimator (L = 2) offers an improvement of approximately two dB over bit by bit detection, [6,7] but the performance improvement in using a more complicated MLSE does not appear in the literature for GTFM or GMSK.

We hope to clear up the uncertainty, (or maybe even add to it), by using GTFM(0.62,0.36), and comparing the results obtained, by simulation, with an optimized differential detector, and an optimized discriminator, both followed by a MLSE of modest complexity (two and four states). (Figures 3.6.1 and 3.6.2 depict the various configurations and detectors to be tested).

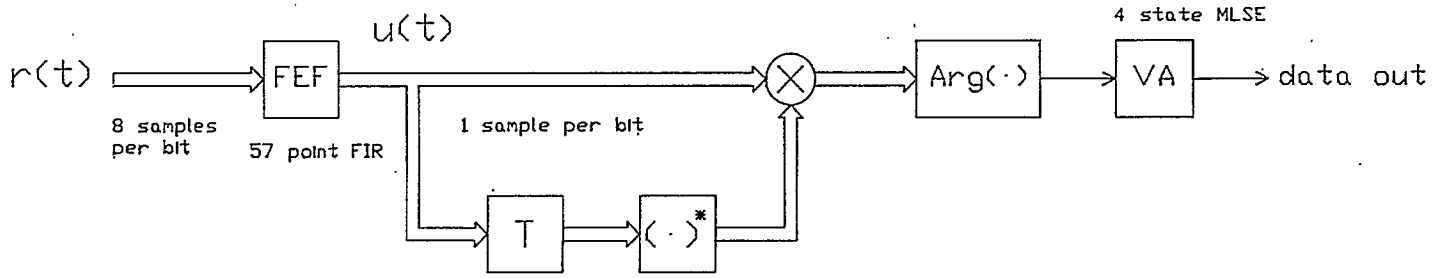

Figure 3.6.1

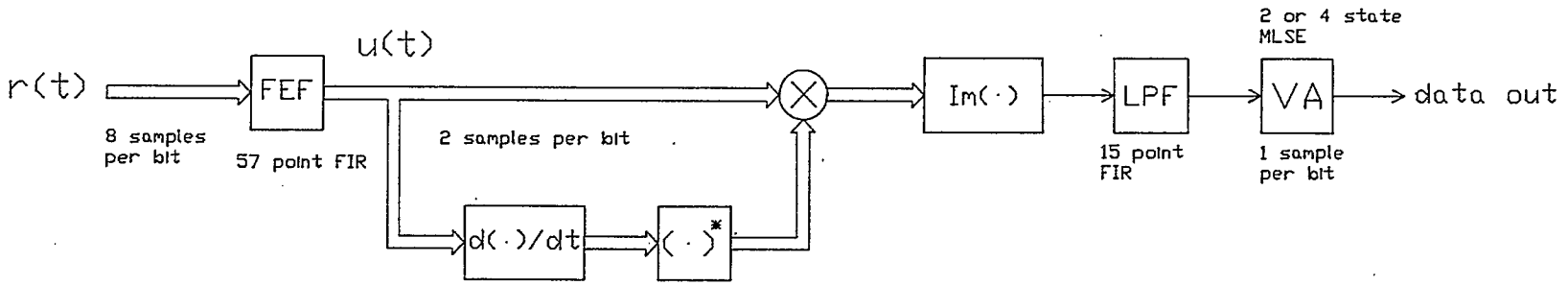

Figure 3.6.2

4. SIMULATION RESULTS FOR STATIC CHANNELS

4.1 Optimization of Front End Filters

While judicious lip service has been paid to addressing the problem of incoherent detection of CPM, (i.e. TFM, GTFM, GMSK), a sensible optimization criterion for front end filters has not been applied. Gaussian front end filters abound in the literature; however, a gaussian filter possesses no criteria of optimality, (except possibly ease of optimization). A more sensible criterion of optimality is minimization of the mean square error (MSE) at the output of the front end filter. (Whether or not this minimizes the average BER is another story). In [7] a gaussian filter was cascaded with a three tap equalizer (with spacing 2T), with good success. Although this is perhaps better than using only a gaussian filter, it still is not optimum in any reasonable sense. (It seems a shame that some people implement modems in hardware, without the advantage of a TMS32010 !)

The scheme used for minimization of the MSE is shown in figure 4.1.1 [21]. The simulation was run at a signal to noise ratio (E_b/N_o) of 7 dB, with the two nearest adjacent channels (5 kHz channel spacing) 13 dB higher than the desired channel. The equalizer was fractionally tapped, with 8 samples per bit, and 57 taps. The equalizer converged to the impulse response shown in figure 4.1.2, (real and complex parts). The frequency responses of the front end filters are shown in figures 4.1.3 and 4.1.4. The front end filter attenuates the adjacent channel by 17 dB at the desired signal's band edge, and by more than 60 dB at the nearest adjacent channel's center, assuming transmission at 4.8 kbps and 5 kHz channel spacing.

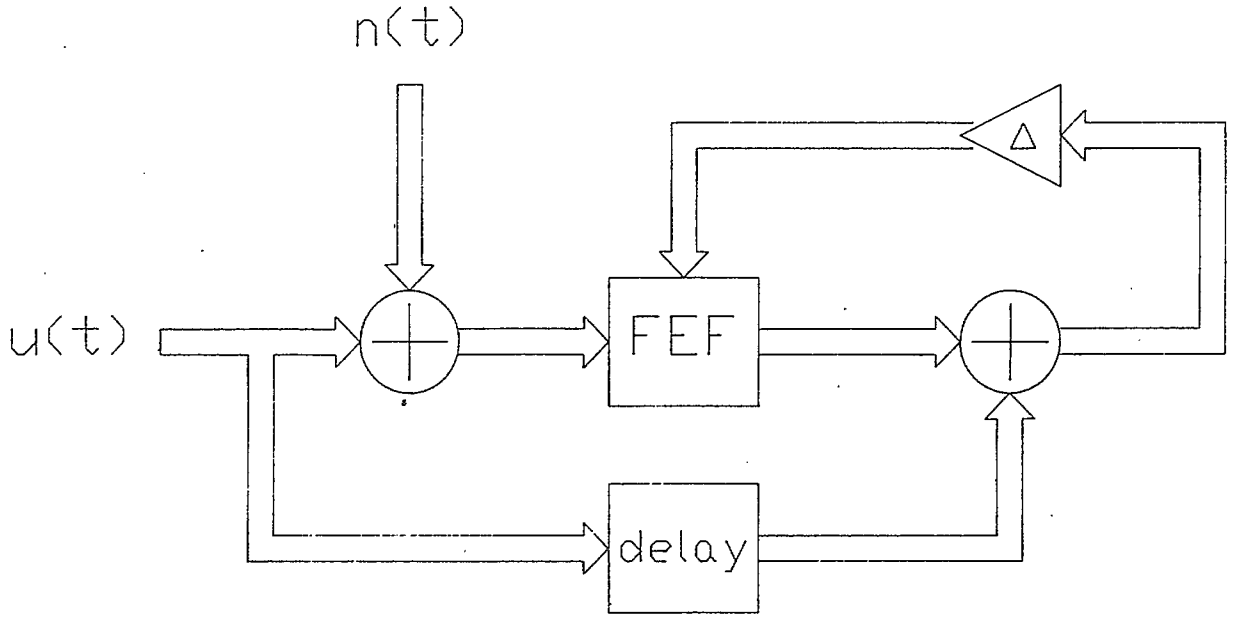

Figure 4.1.1.

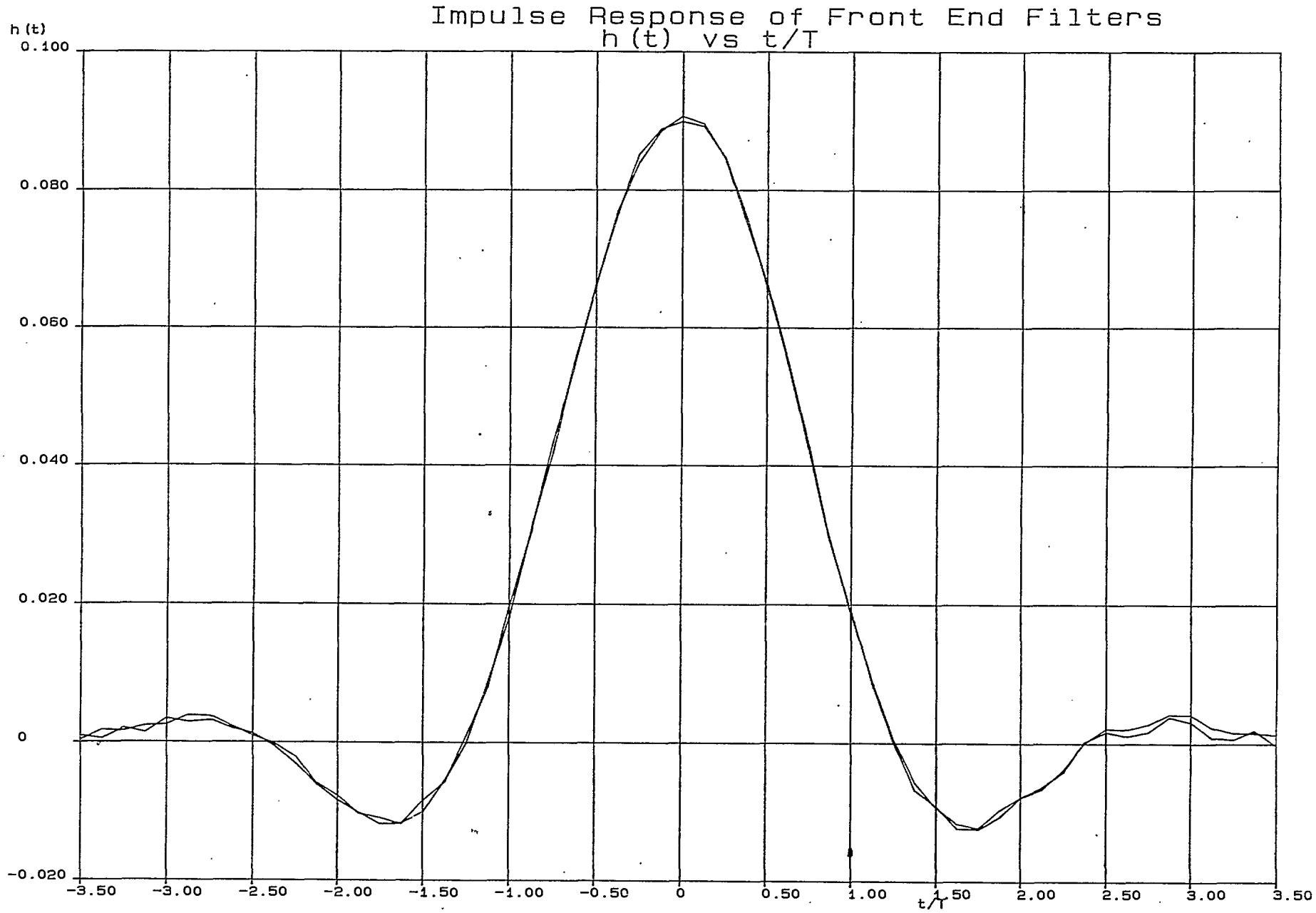
Impulse Response of Front End Filters
h(t) vs t/T
h(t)
0.100
0.080
0.060
0.040
0.020
0
-0.020
-3.50
-3.00
-2.50
-2.00
-1.50
-1.00
-0.50
0
0.50
1.00
1.50
2.00
2.50
3.00
3.50
t/T

Figure 4.1.2

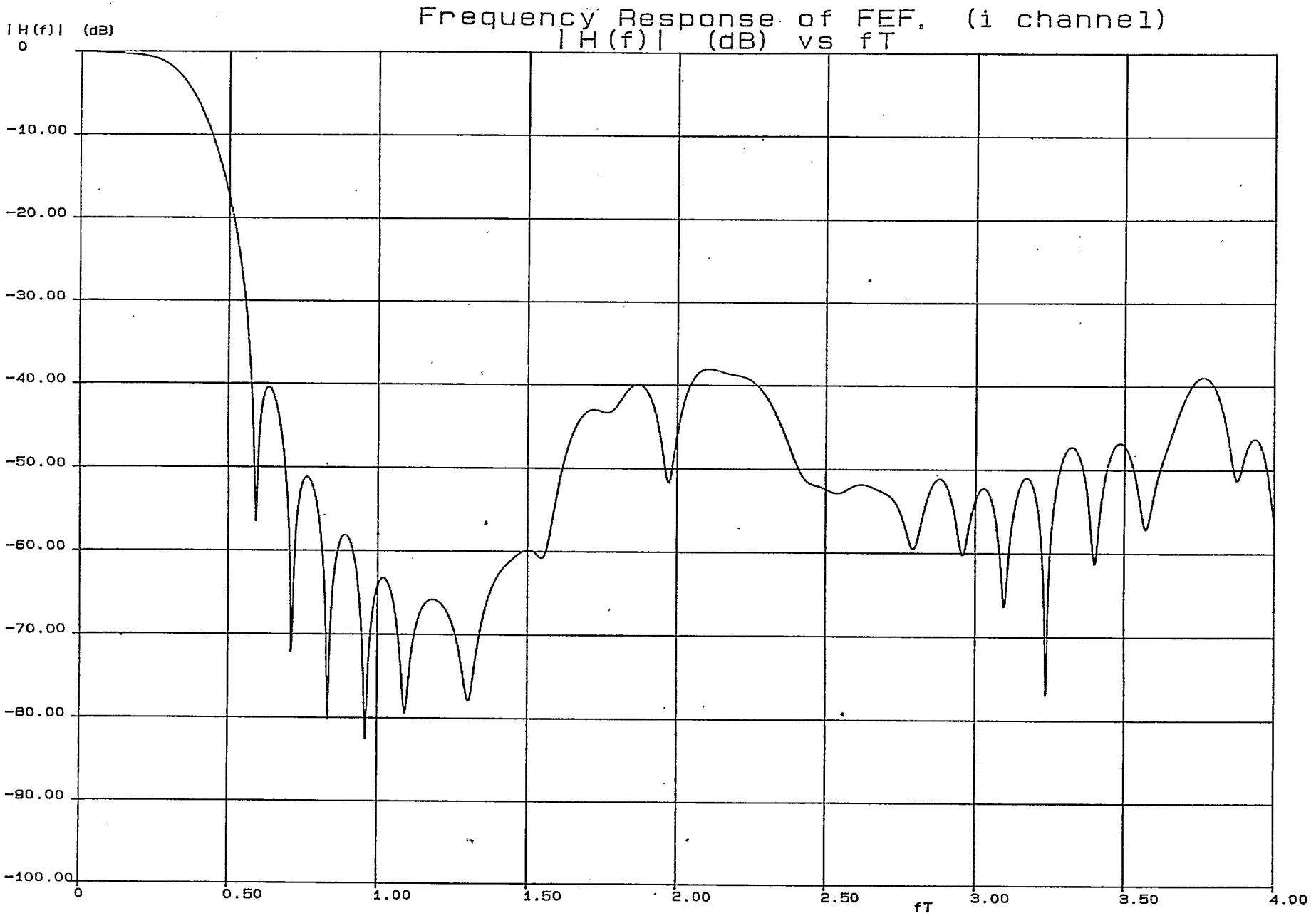
Frequency Response of FEF, (i channel)
|H(f)| (dB) vs fT
|H(f)| (dB)
0
-10.00
-20.00
-30.00
-40.00
-50.00
-60.00
-70.00
-80.00
-90.00
-100.00
0
0.50
1.00
1.50
2.00
2.50
3.00
3.50
4.00
fT

Figure 4.1.3

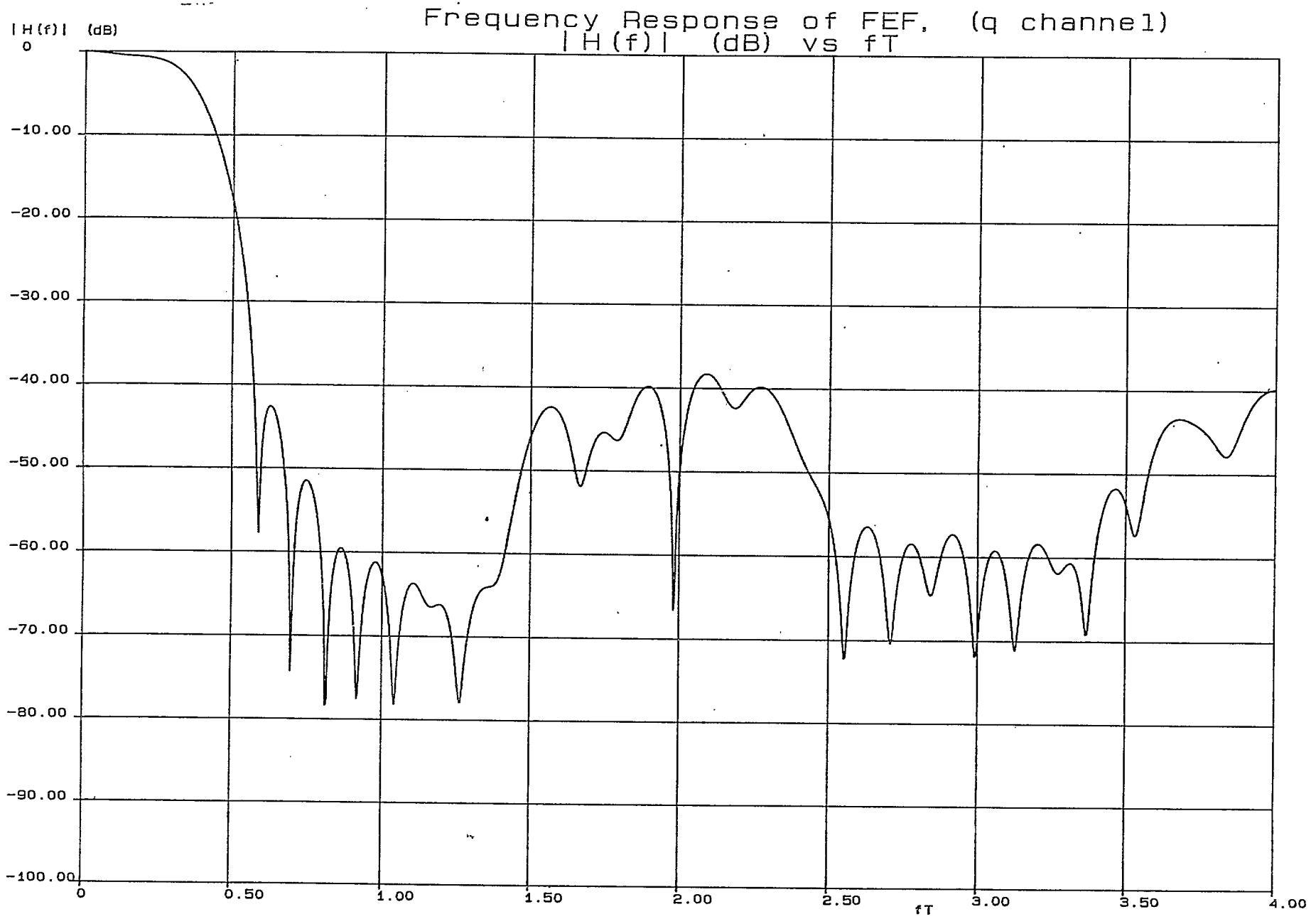
Frequency Response of FEF, (q channel)
|H(f)| (dB) vs fT
|H(f)| (dB)
0
-10.00
-20.00
-30.00
-40.00
-50.00
-60.00
-70.00
-80.00
-90.00
-100.00
0
0.50
1.00
1.50
2.00
2.50
3.00
3.50
4.00
fT

Figure 4.1.4

4.2 Performance of Discriminator Detection

As discussed in section 3.4 the discriminator detector differentiates the phase function of the received complex envelope. A low pass filter follows the differentiation in order to minimize the effects of the multiplication non-linearity. The front end filter (FEF) was discussed in section 4.1. In the simulations, 8 samples per bit were used for the FEF, and two samples per bit used for the low pass filter (LPF). Although two samples per bit may not be adequate, it was decided that using more than 2 samples per bit after the front end filter would result in a system which was not implementable on the TMS320 due to execution time constraints. The low pass filter (FIR, length 15) was optimized using the same method as discussed in section 4.1. The eye diagram of this scheme with no front end filters (figure 4.2.1) and with the optimized front end and low pass filters (figure 4.2.2) displays both the three level eye and six level eye. It must be noted that the six and the three level eye is only good fortune. Recall that the definition of TFM involves a Nyquist-3 pulse which constrains the phase pulse to pass through discrete points yet provides no such constraints on the frequency pulse. That is, a Nyquist-3 pulse does not, in general, pass Nyquist-1. Without filtering, both eyes are very good. However, with the introduction of the FEF and LPF considerable degradation is evident in the three level eye, yet only modest degradation in the six level eye. Notice that the six level eye obeys a different correlative encoding rule when the filters are incorporated.

The correlative encoding rule for the six level eye is:

$$d\hat{\phi}(k,\underline{\alpha})/dt = f*\underline{\alpha}$$

where, (from figure 4.2.2),

$$f = (f_0, f_1, f_2) = (0.215, 0.57, 0.215)$$

Obviously, the correlative encoding rule for the three level eye must

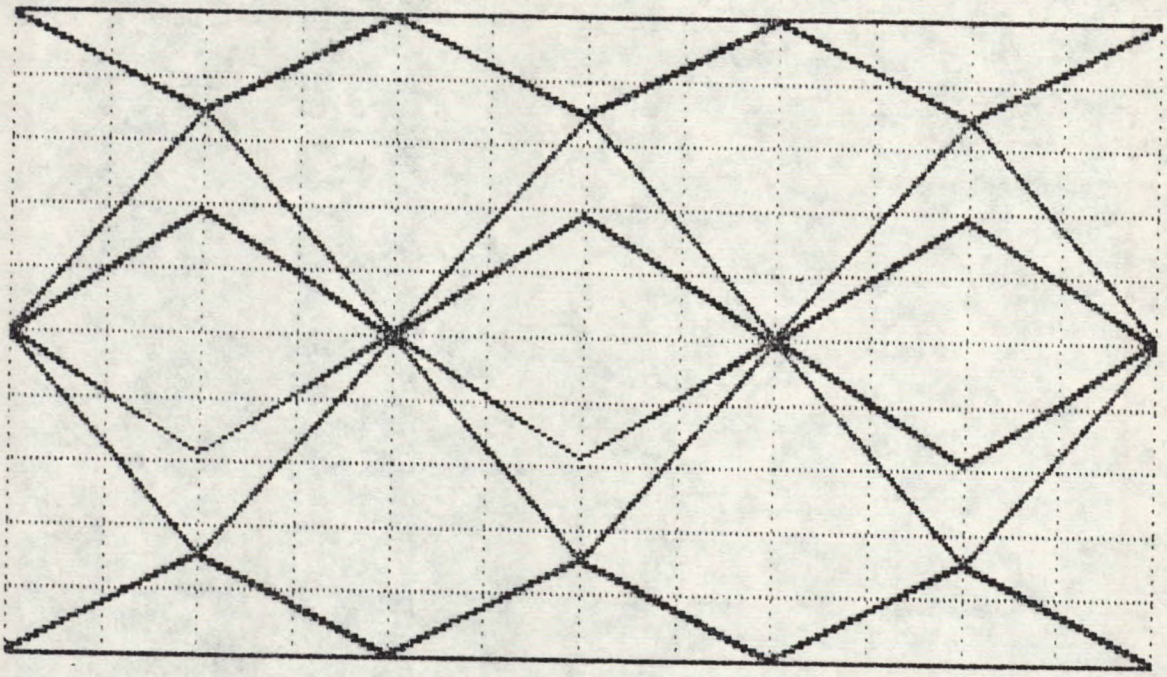

Figure 4.2.1

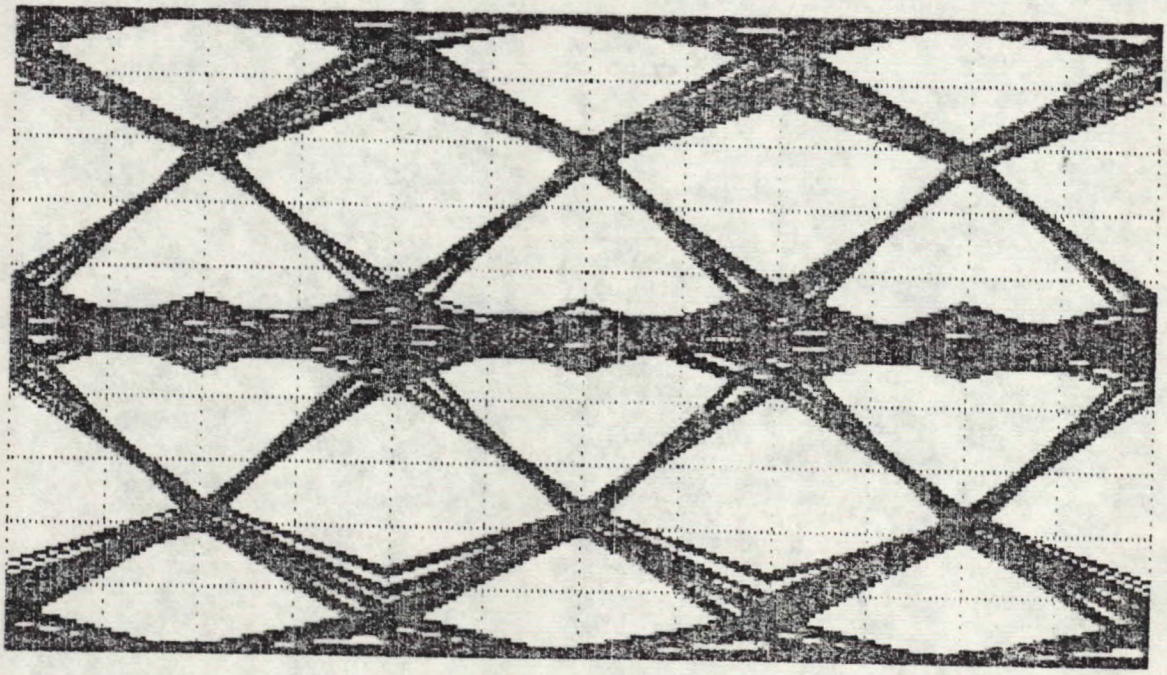

Figure 4.2.2

obey:

$$f = (f_0, f_1) = (0.50, 0.50)$$

Performance using a two and four state MLSE is shown in figure 4.2.3. Perfect timing and no frequency offset is assumed. The more complex four state MLSE provides a gain of approximately 0.8 dB over the two state MLSE at a BER of 10^{-2} and 1.2 dB at a BER of 10^{-3}. The increased complexity seem worth it.

It is interesting to note that [7] (figure 3.5.11) obtained a BER of 10^{-2} at a signal to noise ratio (E_b/N_o) of 8 dB. That is, the two state MLSE simulated here was 0.40 dB poorer than the simulations conducted by [7]. Two possibilities exist for the discrepancy: either minimization of the mean square error is not a good method for optimizing filters, or using two samples per bit after discriminator detection is not adequate. With regard to the first possibility, the filter was optimized with adjacent channels 13 dB higher than the desired channel. Re-optimization without adjacent channels and eight samples per bit after the discriminator (the same used in [7]) should provide us with enough insight to explain the discrepancy. However, rather than belaboring the point, the results from differential detection will be investigated.

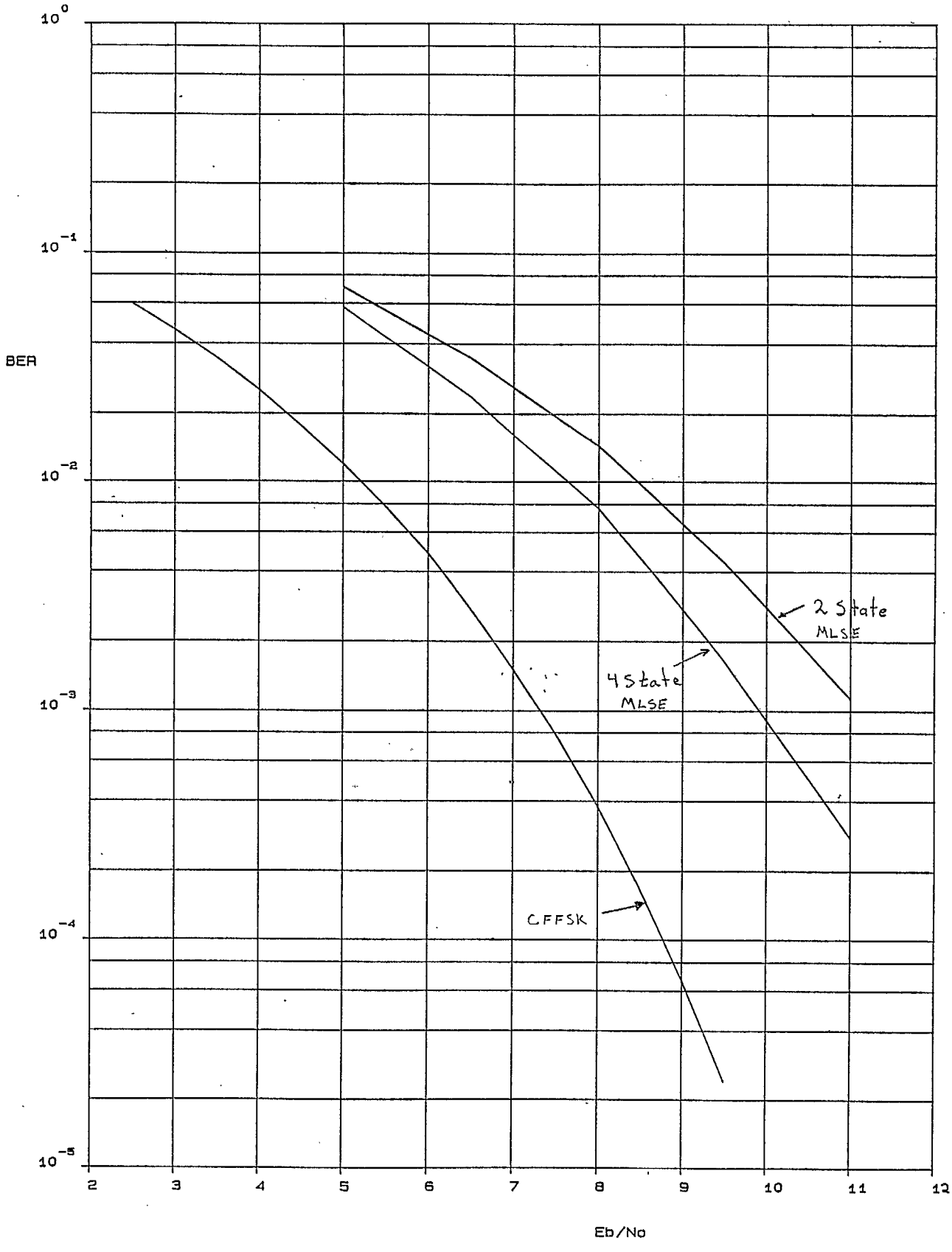
10^{0}
10^{-1}
10^{-2}
10^{-3}
10^{-4}
10^{-5}
BER
2
3
4
5
6
7
8
9
10
11
12
Eb/No
2 State MLSE
4 State MLSE
CFFSK

Figure 4.2.3

4.3 Performance of Differential Detection

In section 3.3 differential detection of CPM was discussed. The FEF used in the simulations was the same as that used for discriminator detection. Simulations were also performed using a low pass filter following the differential phase detector. However, no gain in performance was realized.

The differential eye diagram (using the detector in figure 3.3.2) is shown in figure 4.3.1 for no front end filter and in figure 4.3.2 for the FEF discussed above. The front end filter introduces considerable intersymbol interference into the three level eye, but a fairly clean six level eye remains. (Again, the six level eye obeys a different correlative encoding rule when the FEF is introduced).

The correlative encoding rule for the six level eye is:

$$\hat{\phi}(k,\underline{\alpha}) = \underline{f} * \underline{\alpha}_k$$

where, (from figure 4.3.2),

$$\underline{f} = (f_0, f_1, f_2) = (0.235, 0.53, 0.235)$$

BER performance of differential detection followed by a four state MLSE is shown in figure 4.3.3. Differential detection offers a 0.4 dB improvement over discriminator detection at a BER of 10^{-2} and a 0.60 dB improvement at a BER of 10^{-3} (both with 4 state MLSEs).

Performance of both detectors, and the reference curve CFFSK (coherent Fast FSK) is shown in figure 4.3.4. Differential detection offers BER performance only 2.1 dB poorer than CFFSK.

Performance exceeds that obtained in [7] by 0.70 dB and 1.1 dB at a BER of 10^{-2} and 10^{-3} respectively. Performance gains over optimum incoherent detection of TFM [13] are similar.

Thus the superior performance of the differential detector and the added bonus of only needing to compute front end filter outputs once per

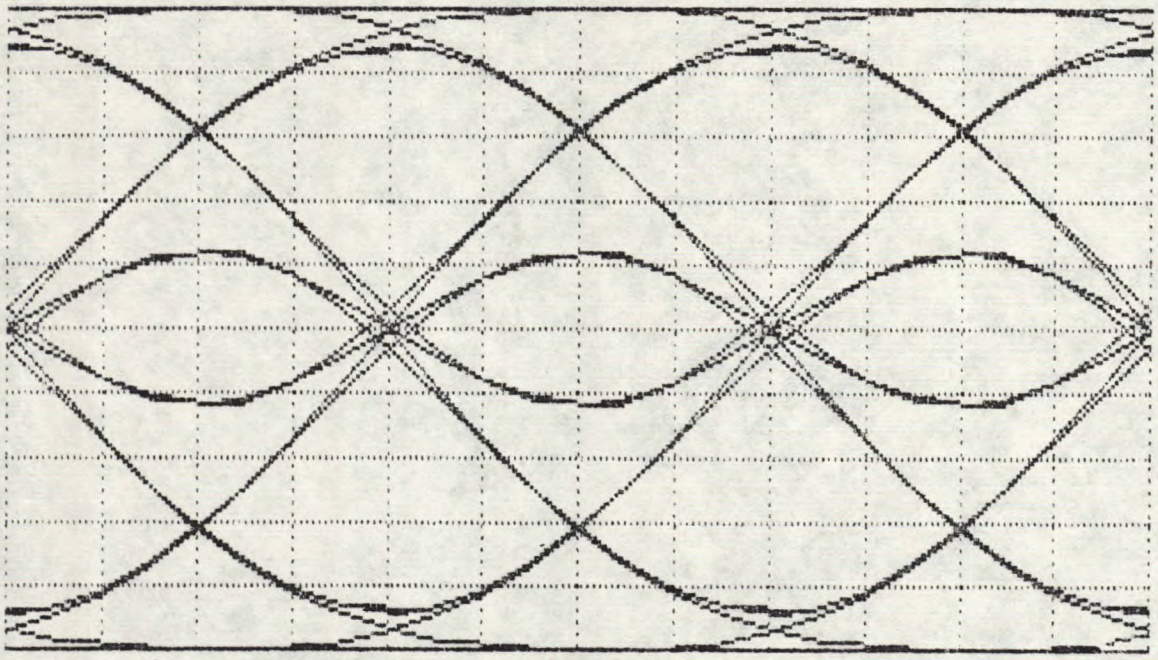

Figure 4.3.1

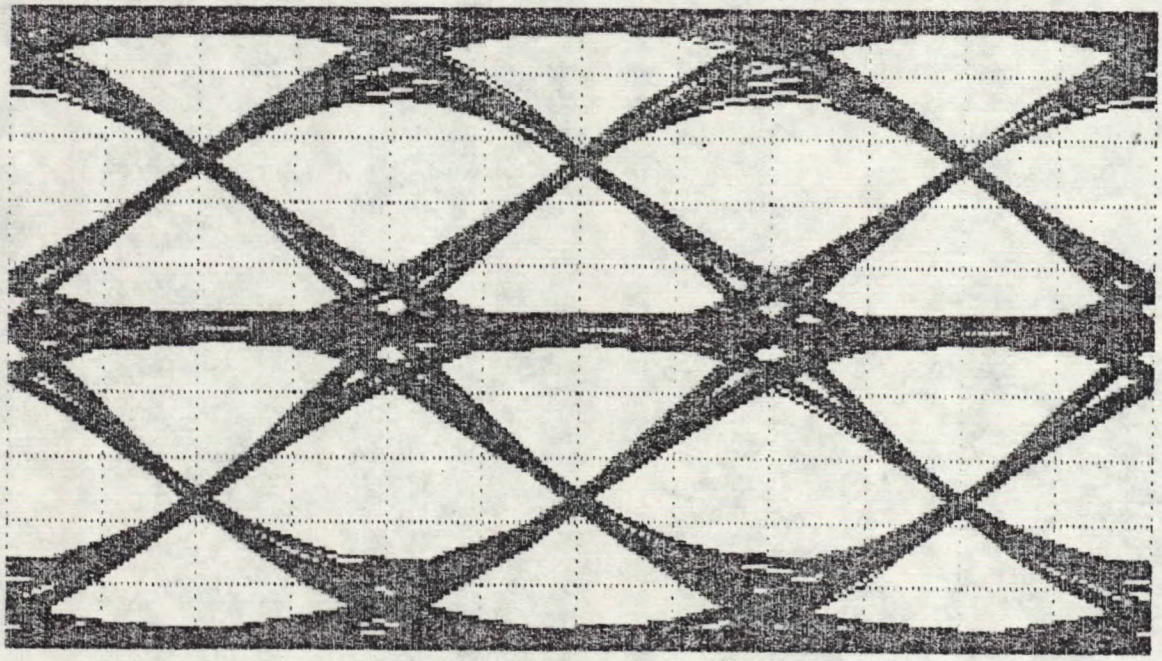

Figure 4.3.2

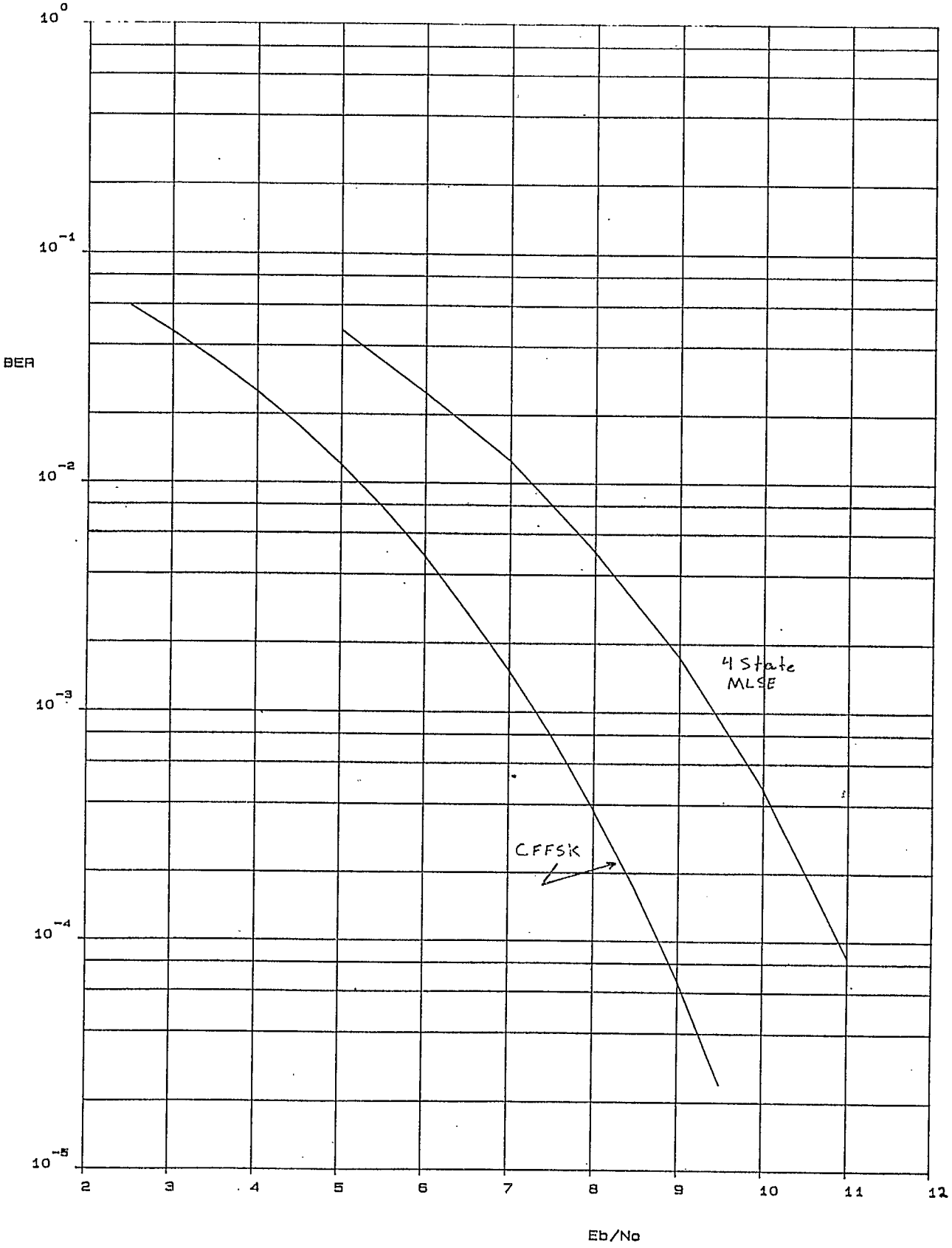
10^{0}
10^{-1}
10^{-2}
10^{-3}
10^{-4}
10^{-5}
BER
2
3
4
5
6
7
8
9
10
11
12
Eb/No
4 State
MLSE
CFFSK

Figure 4.3.3.

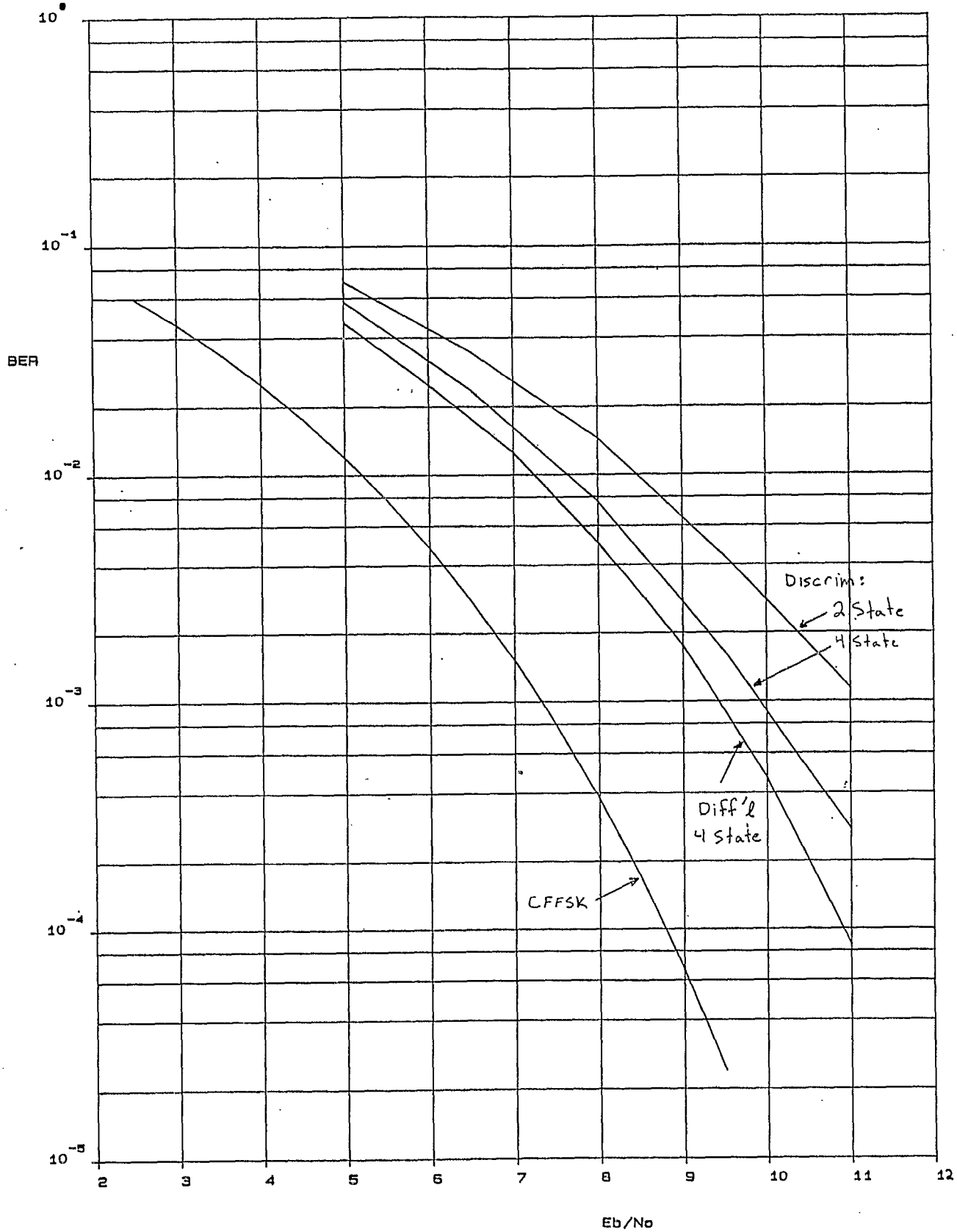
BER
10^{0}
10^{-1}
10^{-2}
10^{-3}
10^{-4}
10^{-5}
2
3
4
5
6
7
8
9
10
11
12
Eb/No
Discrim:
2 State
4 State
Diff'l
4 State
CFFSK

Figure 4.3.4

bit make differential detection the clear winner. A problem exists since an Arg function is necessary, and a timing algorithm utilizing the supplied information (i.e. the FEF outputs) must be developed. However, an Arg function is simple (maybe, if we have a TMS320) and an adequate timing signal is evident upon close inspection of the six level eye, (see section 5.2).

4.4 Effects of Frequency Offsets and Timing Error

The degradation in the performance of differential detection in the presence of frequency offsets, is shown in figure 4.4.1, for various frequency offsets (f_D), (as a percentage of the bitrate).

f_D/R (%)	degradation (dB)
± 0.5	<0.10
± 1.0	0.15
± 1.5	0.25
± 2.0	0.60

Figure 4.4.1

It is apparent the frequency offset should be kept within 1.5 percent of the bitrate (72 Hz), for adequate performance to be maintained.

Thus, our acquisition algorithm should be designed to estimate the frequency offset to within ± 75 Hz with high probability.

The degradation due to timing errors of ± $1/16^{th}$ and ± $1/8^{th}$ of a bit is shown in figure 4.4.2.

timing error (bits)	degradation (dB)
± 1/16	0.10
± 1/8	0.40

Figure 4.4.2

Hence, an accurate bit tracking algorithm with negligible jitter (<$1/16^{th}$ of a bit) is necessary. Also, the acquisition algorithm should

estimate the starting bit timing to less than $1/8^{th}$ of a bit.

4.5 Effects of Adjacent Channels

The bandwidth efficiency of GTFM is demonstrated in figure 4.5.1, in which degradation due to adjacent channels, with various carrier to interferer ratios (C/I), and 5 kHz channel spacing is displayed. The carrier to interferer ratio is defined as the power in the desired channel, divided by the power in a single interfering channel. In the simulations the two nearest adjacent channels were used, both with equal C/I ratios.

C/I (dB)	degradation (dB)
-18.0	1.00
-13.5	0.40
-9.0	0.15
-4.5	< 0.10
0.0	< 0.05

Figure 4.5.1

For the worst case scenario, two adjacent channels, both more than 13 dB higher than the desired channel, the degradation is only 0.40 dB. Thus, the GTFM parameters chosen are more than adequate for the system in study.

Secondly, for the desired channel and two adjacent channels, all of equal power, the degradation is minimal.

4.6 Summary

In this section we have studied, by simulation, discriminator and differential detection, with differential detection providing the best performance, (2.1 dB degradation from CFFSK). It is important to note, (from our perspective), that the differential detector studied actually outperforms differential detection of MSK discussed in [Matayas, no SEC cicuit].

The SEC (single error correcting) circuit could also be utilized, (for differential detection of GTFM), if the differential phase over two bits was also computed [12]. The performance using this technique [12] was promising, and the SEC circuit is much simpler than a MLSE. However, its performance is inferior to the differential detector discussed above. The exact implementation used in [12] was not discussed, and the papers referenced were written in Japanese, (which is not one of the author's stronger languages).

The differential phase over one and two bits could perhaps be better utilized by using one, albeit longer, maximum likelihood sequence estimator. One must remember, though, that tremendous gains cannot be made since the above detector is only 2.1 dB worse than CFFSK.

In any event, the detector chosen has excellent performance provided the frequency offset and initial bit timing are estimated accurately, and the bit timing is tracked adequately.

5. ACQUISITION AND TRACKING

5.1 Acquisition of Frequency and Bit Timing

The modem is to operate in a burst mode, wherein the receiver must resynchronize (in center frequency and bit phase), with the transmitter after idle periods. The technique used in [23] could be used in its entirety, (2400 bps MSK with the dotting pattern ...-1,+1,-1,+1,...). However, the response of the receiver to the remaining MSK pattern upon acquisition might be undesirable. The obvious pattern to use with GTFM(0.62,0.36) is the ...+1,+1,-1,-1,+1,+1,... pattern which has good zero crossings and large amplitude (figure 5.1.1).

The acquisition stage is split up into three smaller stages: detection, comb filtering, and analysis. The detection stage is concerned with detecting the presence of the dotting pattern, the comb filtering stage is concerned with averaging the received signal over M bit periods, and the analysis stage is concerned with calculating the frequency offset and initial bit phase.

Figures 5.1.2 and 5.1.3 illustrates both the detection (synch hunt), and comb filtering stages. In both phases, the received complex envelope is first low pass filtered to exclude most of the out of band noise prior to differential detection.

Recall:

$$r(t) = v(t,\underline{\alpha})\exp(j2\pi f_D t) + n(t)$$

where

f_D is the center frequency offset, and

$\underline{\alpha}$ = ...+1,+1,-1,-1,+1,+1,-1,-1,...

After low pass filtering:

$$r'(t) = r(t)*h(t)$$

$$= (v(t,\underline{\alpha})\exp(j2\pi f_D t))*h(t) + n(t)*h(t)$$

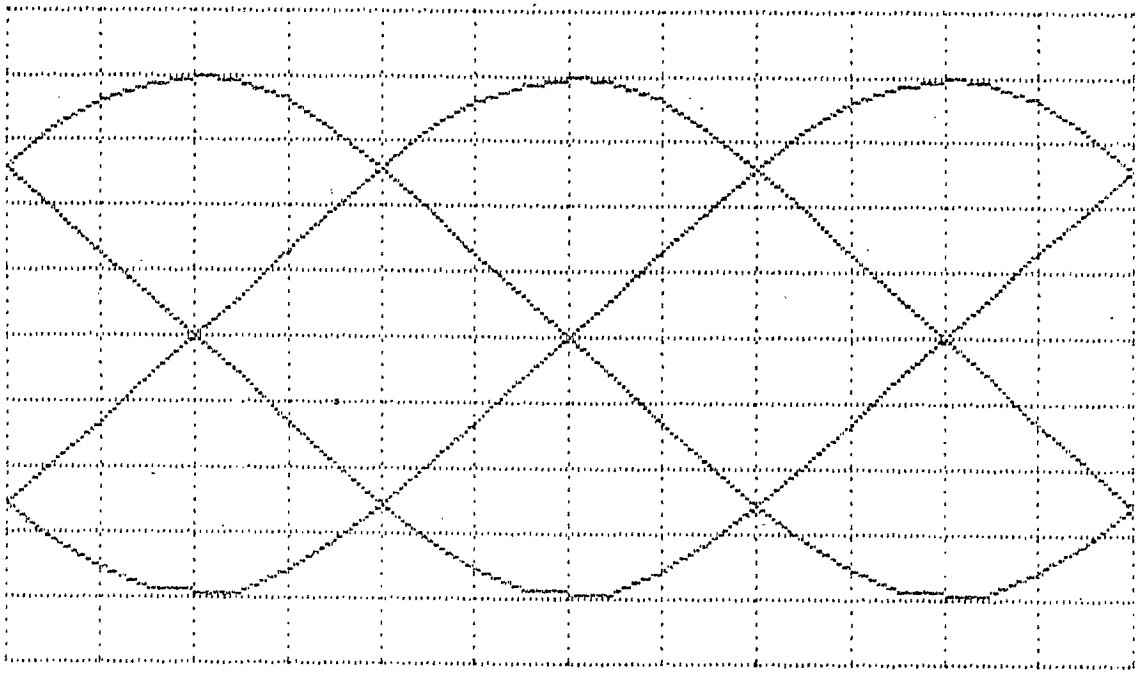

Figure 5.1.1.

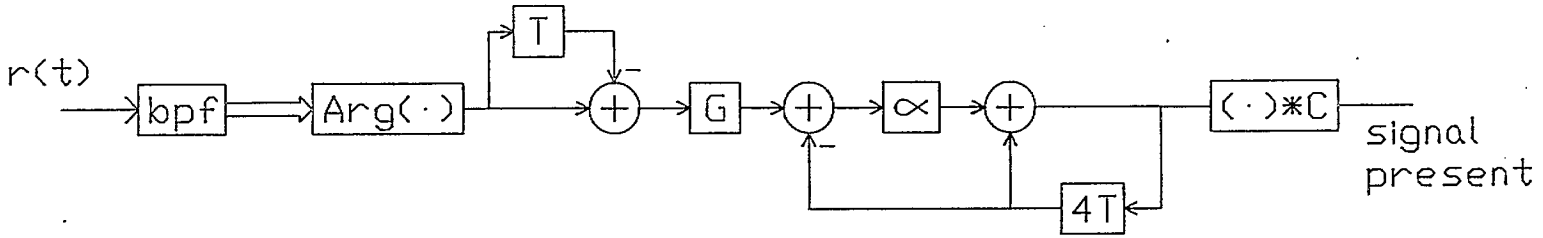

Figure 5.1.2

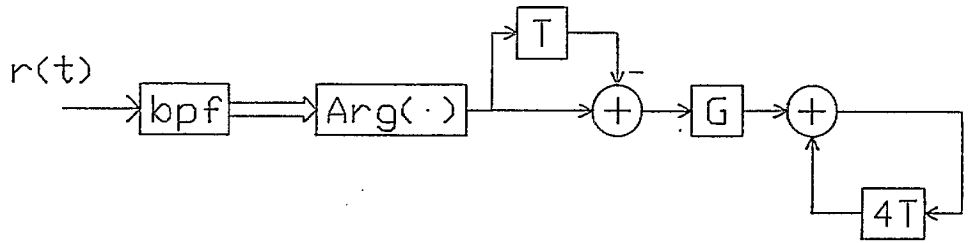

Figure 5.1.3

$$= v'(t,\underline{\alpha}) + n'(t)$$

We note that $v(t,\underline{\alpha})$ is periodic with period 4T but loses its periodic nature due to the frequency shift. Periodicity is restored in the differential detector, which is stepped twice per bit.

After differential detection we have:

$$\text{Arg}(v'(t,\underline{\alpha})v'^{*}(t,\underline{\alpha})\exp(j2\pi f_D T) + \text{noise terms})$$

$$= 2\pi f_D T + \text{Arg}(v'(t,\underline{\alpha})v'^{*}(t,\underline{\alpha}) + \text{noise terms})$$

We note that the frequency offset introduces a shift in the received differential phase.

During the detection phase the differentially detected signal y(t) is first comb filtered, and correlated against a signal which would be received in the absence of noise. When the output of the correlator rises above a threshold, the signal is assumed to be present and the analysis stage is entered.

During the comb filtering portion, the comb memory is extended to infinity (a pure averager), and once M bits have been processed the average level in the comb buffer determines the frequency offset, and the zero crossing after correlation with a clean signal dtermines the bit clock phase, (analysis section).

Simulations have shown that with M=128, a preamble length of 250 bits (52 msec), was necessary to obtain frequency offset estimates within 30 Hz of the actual frequency offset with 95% probability and bit phase estimates within $1/16^{th}$ of a bit with 95% probability at a signal to noise ratio (E_b/N_o) of 7 dB. Although this is better than we previously stated we require, the performance at lower signal to noise ratios and larger frequency offsets may still be acceptable.

5.2 Bit Tracking in Demod Mode

Although the popular bit tracking schemes such as the filter-square bit synchronizer [24], early late gate synchronizer, and numerous others [25], would work quite well, the number of cycles needed to implement these algorithms is large. A timing error signal was derived by careful examination of the six level eye. The differential phase at the output of the differential detector can be approximated by:

$$\hat{\phi}(k,\hat{\underline{\alpha}}) = f_2\hat{\alpha}_{k-2} + f_1\hat{\alpha}_{k-1} + f_0\hat{\alpha}_k$$

If we observe a change in sign between $\hat{\alpha}_k$ and $\hat{\alpha}_{k-2}$, then we should observe:

$$y_k = f_1\alpha_{k-1} + n_k$$

With a small timing error, (τ), we would observe:

$$y_k = f_1\alpha_{k-1} + \delta(\tau)\alpha_k + n_k$$

Our timing error is just:

$$t_k = y_k - f_1\alpha_{k-1}$$

$$= \delta(\tau)\alpha_k + n_k$$

For small τ, $\delta(\tau) \approx k\tau$

By using decision feedback to estimate the α_k's and by averaging the t_k's we can arrive at a good and consistent estimate of the timing error.

The timing algorithm is shown in figure 5.2.1. Thus, in order to make an appropriate decision on the timing error, we average the t_k's in a first order lowpass filter, and bump the phase of the sampling clock depending on the sign of the filter output.

Simulation studies have shown that this algorithm performs well at a signal to noise ratio (E_b/N_o) of 7 dB. An appropriate value of α to minimize jitter while maintaining acceptable tracking performance will be choosen once the modem is implemented on a TMS32010.

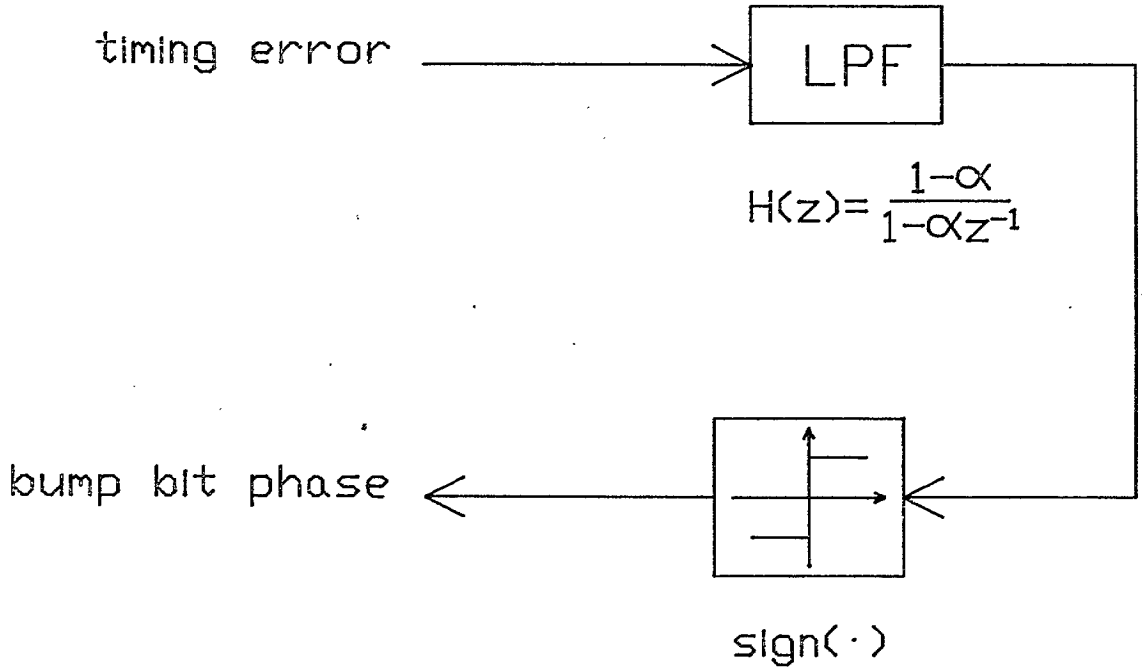
timing error
LPF
$H(z)=\frac{1-\alpha}{1-\alpha z^{-1}}$
bump bit phase
sign(·)

Figure 5.2.1

6. CONCLUSIONS

This document discussed the development of a modem designed to operate at 4800 bps over an MSAT channel. The prototype implementation gives excellent performance, within measurement error of the values predicted by simulation.

The modem is to interface to a 4.8 kHz IF, and the channels are assumed to be spaced 5 kHz apart. A companion report entitled "A 4800 bps GTFM Modem, Part 2- Implementation and Performance Tests", discusses the implementation of the modem on a TMS320 digital signal processor and the corresponding hardware tests.

The results are satisfying. We met MSAT requirements; in fact the performance is better than any results quoted in the literature for practicable demodulation methods. Moreover, the results time scale to demonstrate the possibility of 24 kbps with standard land mobile 25 kHz channel spacing. Finally, the implementation rests on a general purpose DSP chip, so it does not suffer from problems of drift, aging, and other analog ailments.

Based on previous analysis and simulation, and the reported implementation and performance tests discussed above, we state, in summary form, our main technical results:

1. We investigated two incoherent detection structures - discriminator and differential - using simulation. The structures were similar: front end filter for adjacent channel and out of band noise rejection, detector, post detection lowpass (except for the differential detector) and Viterbi algorithm.
2. We designed the front end and post detection filters simply by running an adaptive filter, in the worst case noise and adjacent channel interference conditions, to minimize mean squared error.

3. The presence of the front end filter caused blurring of the post detector eye diagrams, and in some cases, an outright separation of the levels. We compensated by approximating the eyes with an experimentally derived encoding polynomial in the Viterbi Algorithm.
4. In the discriminator detector, the 6 level eye (nominal 5) was less smeared than the nominal 3 level eye. We found that a 4 state VA used on the 6 level eye gave between 0.8 and 1.2 dB better performance than a 2 state VA on the 3 level eye.
5. The discriminator detector was 0.4 dB worse than a result in the literature for a 2 state VA which was unhampered by the tight front end filter we need for adjacent channel rejection.
6. The differential detector with its 6 level eye (nominal 5 level) and 4 state VA was 0.4 to 0.6 dB better than the equivalent discriminator detector, and 0.7 to 1.1 dB better than both the best previously reported results in the literature for this class of detector and optimum incoherent TFM with an 8 bit window.
7. Degradation due to parameter error for the 4 state differential detector is: 0.60 dB for 2 per cent frequency offset; 0.4 dB for sample time error of 0.125 symbol duration; 0.4 dB for both adjacent channels 13.5 dB higher than the desired channel.
8. The DSP chip loading of the differential detector was also better than the differential detector, so we adopted it.

REFERENCES

[1] T. Aulin and C.W. Sundberg, "Continuous Phase Modulation-Part I: Full Response Signaling", *IEEE Trans. Commun.*, Vol COM-29, No. 3, pp. 196-209, March 1981.

[2] ----, "Continuous Phase Modulation-Part II: Partial Response Signaling", *IEEE Trans. Commun.*, Vol COM-29, No. 3, pp. 210-225, March 1981.

[3] R. de Buda, "Coherent Demodulation of Frequency-Shift Keying With Low Deviation Ratio", *IEEE Trans. Commun.*, pp. 429-435, June 1972.

[4] W.P. Osborne and M.B. Luntz, "Coherent and Noncoherent Detection of CPFSK", *IEEE Trans. Commun.*, Vol. COM-22, No. 8, pp. 1023-1037, Aug. 1974.

[5] F. de Jager and C.B. Dekker, "Tamed Frequency Modulation, A Novel Method to Achieve Spectrum Economy in Digital Transmission", *IEEE Trans. Commun.*, Vol COM-26, No. 5, pp. 534-542, Nov. 1975.

[6] K.S. Chung and L.E. Z egers, "Generalized Tamed Frequency Modulation", *Philips Telecommunication Review*, Vol. 41, No. 1, pp 82-91, April 1983.

[7] K.S. Chung, "Generalized Tamed Frequency Modulation and Its Application for Mobile Radio Communications", *IEEE Journal on Sel. Areas of Commun.*, Vol. SAC-2, No. 4, pp. 487-497, July 1984.

[8] U. Wellens, "Transmission Performance of Tamed Frequency Modulation In UHF Mobile Telephone Systems", *Proc. IEEE Int'l Conf. Commun.*, pp. B8.2.1-5, Boston 1983.

[9] S. Elnoubi and S.C. Gupta, "Error Rate Performance of Noncoherent Detection of Duobinary Coded MSK and TFM in Mobile Radio Communication Systems", *IEEE Trans. Vehic. Tech.*, Vol. VT-30, No. 2, pp. 62-76, May 1981.

[10] K. Murota and K. Hirade, "GMSK Modulation for Digital Mobile Radio Telephony", *IEEE Trans. Commun.*, Vol. Com-29, No. 7, pp. 1044-1050 July 1981.

[11] K. Daikoku, K. Murota, and K. Momma, "High-Speed Digital Transmission Experiments in 920 Mhz Urban and Suburban Mobile Radio Channels", *IEEE Trans. Vehic. Tech.*, Vol. VT-31, No. 2, pp. 70-75, May 1982.

[12] K. Kinoshita, M. Hata, and H. Nagabuchi, "Evaluation of 16 kbits/s Digital Voice Transmission for Mobile Radio", *IEEE Trans. on Vehic. Tech.*, Vol. VT-33, No. 4, pp. 321-327, Nov. 1984.

[13] D. Muilwijk, "Correlative Phase Shift Keying- A Class of Constant Envelope Modulation Techniques", *IEEE Trans. Commun.*, Vol COM-29, No. 3, pp. 226-236, March 1981.

[14] P.J. McLane, "The Viterbi Reciever for Correlative Encoded MSK Signals", *IEEE Trans. Commun.*, Vol. COM-31, No. 2, pp. 290-295, Feb. 1983.

[15] R.R. Anderson, W.R. Bennett, J.R. Davey, and J. Salz, "Differential Detection of Binary FM", *Bell System Tech. Journ.*, pp. 111-159, January 1965.

[16] A.J. Viterbi, "Error Bounds for Convolutional Codes and an Asymptotically Optimum Decoding Algorithm", *IEEE Trans. Inform. Theory*, Vol. IT-13, pp. 260-269, April 1967.

[17] G.D. Forney Jr., "Maximum-Likelihood Sequence Estimation of Digital Sequences in the Presence of Intersymbol Interference", *IEEE Trans. on Info. Theory*, Vol IT-18, No. 3, pp. 363-378, May 1972.

[18] G.D. Forney, Jr., "The Viterbi Algorithm", *Proc. of the IEEE*, Vol. 61, No. 3, pp 268-278, March 1973.

[19] H. Kobayashi, "Correlative Level Coding and Maximum-Likelihood Decoding", *IEEE Trans. on Info. Theory*, Vol. IT-17, No. 5, pp 586-594,

Sept. 1971.

[20] M.J. Ferguson, "Optimal Reception for Binary Partial Response Channels", *Bell System Tech. Journ.*, pp. 493-505, Feb. 1972.

[21] J.G. Proakis, *Digital Communications*, McGraw Hill, 1983.

[22] Jakes, *Microwave Mobile Communications*, John Wiley, 1976.

[23] J.K. Cavers and W.P. LeBlanc, "A 2400 BPS MSK Modem Based on Digital Signal Processing Techniques", under DSS Contract Number 25ST.36100-4-4156, May 1985.

[24] M.K. Simon and C.C. Wang, "Bit Synchronization of Differentially Detected MSK and GMSK", *Proc. IEEE Globecom*, pp 18.7.1-18.7.8, 1985.

[25] R.D. Gitlin and J. Salz, "Timing Recovery in PAM Systems", *Bell System Tech. Journ.*, pp. 1615-1669, May-June 1971.

[26] A.V. Oppenheim and R.W. Schafer, *Digital Signal Processing*, Prentice-Hall, 1975.

APPENDIX A.

THE VITERBI ALGORITHM

VITERBI ALGORITHM

The Viterbi Algorithm is a maximum likelihood sequence estimator (MLSE) which makes optimum sequence decisions on correlative encoded data.

We have:

$$y_k = \sum_{n=0}^{L-1} f_n \alpha_{k-n} + n_k$$

where

the α_k are uncorrelated binary data symbols,

$\underline{f}$ is the sampled impulse response of the channel, (length L),

and the n_k are independent identically distributed gaussian random variables.

Define:

$$c_k = \sum_{n=0}^{L-1} f_n \alpha_{k-n}$$

For $\underline{f}$ spanning L symbols, we have at most 2^L distinct c_k values.

We define s_k as the state of the system, which depends on the last L-1 binary input values.

That is:

$$s_k = [\alpha_k, \alpha_{k-1}, \ldots, \alpha_{k-L+2}, \alpha_{k+1-L}]$$

thus, we have $N = 2^{L-1}$ states.

and:

$$c_k = C(\alpha_k, s_{k-1}) = \sum_{n=0}^{L} f_n \alpha_{k-n}$$

The state at time k+1 depends only on the current state at time k, and the next input value α_{k+1}. That is, we have a first order Markov process, and each state has only two possible successors.

define:

$$s_k^0 = [+1, +1, \ldots, +1, +1, +1]$$

$$s_k^1 = [+1, +1, \ldots, +1, +1, -1]$$

$$s_k^2 = [+1, +1, \ldots, +1, -1, +1]$$

$s_k^{2L-2} = [-1,-1,\ldots,-1,-1,+1]$

$s_k^{2L-1} = [-1,-1,\ldots,-1,-1,-1]$

By defining the states in this way, we observe that the if the current state at time k is (s_k^i) then the previous state was just:

$(2\cdot i) \bmod N$ if $\alpha_{k+1-L} = +1$

$(2\cdot i+1) \bmod N$ if $\alpha_{k+1-L} = -1$

Example $L = 3$, $(N = 2^{L-1} = 4)$

$s_k^i = (\alpha_k, \alpha_{k-1})$

$s_k^0 = (+1,+1)$

$s_k^1 = (+1,-1)$

$s_k^2 = (-1,+1)$

$s_k^3 = (-1,-1)$

The state transition table is,

current state (s_k^i)	previous state (s_{k-1}^i)	$\alpha_k, \alpha_{k-1}, \alpha_{k-2}$
s_k^0	s_{k-1}^0	+1,+1,+1
s_k^0	s_{k-1}^1	+1,+1,-1
s_k^1	s_{k-1}^2	+1,-1,+1
s_k^1	s_{k-1}^3	+1,-1,-1
s_k^2	s_{k-1}^0	-1,+1,+1
s_k^2	s_{k-1}^1	-1,+1,-1
s_k^3	s_{k-1}^2	-1,-1,+1
s_k^3	s_{k-1}^3	-1,-1,-1

We note that if we are currently in state i then the previous state was $2\cdot i \bmod N$ if $\alpha_{k-L+1} = +1$ and $(2\cdot i+1) \bmod N$ if $\alpha_{k-L+1} = -1$, as was mentioned above.

The receiver which minimizes the probability of error for the sequence decision chooses that sequence of α_ks which minimizes:

$$\sum_{k=0}^{\infty} (y_k - C(\alpha_k, s_{k-1}))^2$$
$$= \sum_{k=0}^{\infty} y_k^2 - 2\sum_{k=0}^{\infty} y_k C(\alpha_k, s_{k-1}) + \sum_{k=0}^{\infty} C(\alpha_k, s_{k-1})^2$$

The first sum does not depend on the α_ks. Thus, the optimum receiver chooses the sequence of α_ks which maximizes:

$$2\sum_{k=0}^{\infty} y_k C(\alpha_k, s_{k-1}) - \sum_{k=0}^{\infty} C(\alpha_k, s_{k-1})^2$$

For all those paths with $s_m = [+1,+1,\ldots,+1,+1] = s_m^0$ we may write (1) as:

$$2\sum_{k=0}^{m} y_k C(\alpha_k, s_{k-1}) - \sum_{k=0}^{m} C(\alpha_k, s_{k-1})^2$$
$$+ 2\sum_{k=m+1}^{\infty} y_k C(\alpha_k, s_{k-1}) - \sum_{k=m+1}^{\infty} C(\alpha_k, s_{k-1})^2$$

Thus, any path with $s_m = s_m^0$, and which maximizes (1) also maximizes the first sum. But the first sum only depends on α_0, α_1, α_{m-L}, and s_m and can be chosen independently of the rest of the path.

Define:

$$\mu_k^i = \max \text{ all paths to } s_k^i \quad \sum_{m=0}^{k} 2y_m C(\alpha_m, s_{m-1}) - C(\alpha_m, s_{m-1})^2$$

We call μ_k^i the metric for state s_k^i. We have N states, N metrics, and N best paths to each state. When the paths merge, that is, all best paths agree on the same bit, we may release the bit.

We noted previously that each state has precisely two predecessors, and two successors. Thus, each metric μ_k at state s_k depends on the previous state. Hence, we may write:

$$\mu_k^i = \max \quad \mu_{k-1}^p + 2y_k C(\alpha_k, s_{k-1}^p) - C(\alpha_k, s_{k-1}^p)^2$$
$$\mu_{k-1}^{p+1} + 2y_k C(\alpha_k, s_{k-1}^{p+1}) - C(\alpha_k, s_{k-1}^{p+1})^2$$

for $i = 0,1,\ldots,N-1$

where

$p = 2 \cdot i$ modulo N

and

α_k = +1 for i = 0,1,...,N/2 - 1, -1 otherwise

Case I, L = 2, symmetrical impulse response

We have:

$$C(\alpha_k, s_{k-1}) = 1/2\ (\alpha_k + \alpha_{k-1})$$

With two states ($N = 2^{L-1} = 2$) we must compute:

$$\mu_k^0 = \max \begin{matrix} \mu_{k-1}^0 + 2y_k C(+1, s_{k-1}^0) - C(+1, s_{k-1}^0)^2 \\ \mu_{k-1}^1 + 2y_k C(+1, s_{k-1}^1) - C(+1, s_{k-1}^1)^2 \end{matrix}$$

$$\mu_k^1 = \max \begin{matrix} \mu_{k-1}^0 + 2y_k C(-1, s_{k-1}^0) - C(-1, s_{k-1}^0)^2 \\ \mu_{k-1}^1 + 2y_k C(-1, s_{k-1}^1) - C(-1, s_{k-1}^1)^2 \end{matrix}$$

but:

$$s_{k-1}^i = (\alpha_{k-1})$$

$$s_{k-1}^0 = (+1)$$

$$s_{k-1}^1 = (-1)$$

and:

$$C(+1, s_{k-1}^0) = +1$$

$$C(+1, s_{k-1}^1) = 0$$

$$C(-1, s_{k-1}^0) = 0$$

$$C(-1, s_{k-1}^1) = -1$$

Thus:

$$\mu_k^0 = \max \begin{matrix} \mu_{k-1}^0 + 2y_k - 1 \\ \mu_{k-1}^1 \end{matrix}$$

$$\mu_k^1 = \max \begin{matrix} \mu_{k-1}^0 \\ \mu_{k-1}^1 - 2y_k - 1 \end{matrix}$$

Note that each metric has a corresponding state and best path associated with that state. We define the best path to state s_k^i as:

Γ_k^i = best path to state i.

$= \alpha_k, \alpha_{k-1}, \alpha_{k-2}, \ldots$

Thus, the algorithm for the maximum likelihood sequence estimator is as follows: (|| implies sequence concatenation)

if $\mu^1_{k-1} - \mu^0_{k-1} - 2y_k < -1$

then

$\mu^0_k = \mu^0_{k-1} + 2y_k - 1$

else

$\mu^0_k = \mu^1_{k-1}$

$\Gamma^0_k = \Gamma^1_{k-1}$

if $\mu^1_{k-1} - \mu^0_{k-1} - 2y_k > 1$

then

$\mu^1_k = \mu^1_{k-1} - 2y_k - 1$

else

$\mu^1_k = \mu^0_{k-1}$

$\Gamma^1_k = \Gamma^0_{k-1}$

$\Gamma^0_k = +1 \,||\, \Gamma^0_{k-1}$

$\Gamma^1_k = -1 \,||\, \Gamma^1_{k-1}$

Clearly, it is impossible that both the above inequalities hold. Thus, we may rewrite the algorithm as:

if $\mu^1_{k-1} - \mu^0_{k-1} - 2y_k < -1$

then

$\mu^0_k = \mu^0_{k-1} + 2y_k - 1$

$\mu^1_k = \mu^0_{k-1}$

$\Gamma^1_k = \Gamma^0_{k-1}$ { both paths are equal }

else

if $\mu^1_{k-1} - \mu^0_{k-1} - 2y_k > 1$

then

$\mu^1_k = \mu^1_{k-1} - 2y_k - 1$

$\mu^0_k = \mu^1_{k-1}$

$\Gamma_k^0 = \Gamma_{k-1}^1$ (both paths are equal)

else

$\mu_k^1 = \mu_{k-1}^0$

$\mu_k^0 = \mu_{k-1}^1$

$\Gamma_k^0 = \Gamma_{k-1}^1$ (paths still differ)

$\Gamma_k^1 = \Gamma^0{}_{k-1}$

$\Gamma_k^0 = +1 \;||\; \Gamma_{k-1}^0$

$\Gamma_k^1 = -1 \;||\; \Gamma_{k-1}^1$

Define:

$\mu_k = \mu_k^1 - \mu_k^0$

And the algorithm is as follows:

if $\mu_{k-1} - 2y_k < -1$

then

$\mu_k = -2y_k + 1$

$\Gamma_k^1 = \Gamma^0{}_{k-1}$ (both paths are equal)

else

if $\mu_{k-1} - 2y_k > 1$

$\Gamma_k^0 = \Gamma_{k-1}^1$ (both paths are equal)

then

$\mu_k = -2y_k - 1$

else

$\mu_k = \mu_{k-1}$

$\Gamma_k^0 = \Gamma_{k-1}^1$ (paths still differ)

$\Gamma_k^1 = \Gamma^0{}_{k-1}$

$\Gamma_k^0 = +1 \;||\; \Gamma_{k-1}^0$

$\Gamma_k^1 = -1 \;||\; \Gamma_{k-1}^1$

Bits may be released when both paths agree on the identity of a bit.

Case II, L = 3, symmetrical impulse response

We have:

$$C(\alpha_k, s_{k-1}) = (f_0\alpha_k + f_1\alpha_{k-1} + f_2\alpha_{k-2})$$

and

$$f_0 = f_2,\ f_0 + f_1 + f_2 = 1$$

With four states ($N = 2^{L-1} = 4$) we must compute four metrics,

$$\mu_k^0 = \max \quad \beta_0 = \mu_{k-1}^0 + 2y_kC(+1, s_{k-1}^0) - C(+1, s_{k-1}^0)^2$$

$$\beta_1 = \mu_{k-1}^1 + 2y_kC(+1, s_{k-1}^1) - C(+1, s_{k-1}^1)^2$$

$$\mu_k^1 = \max \quad \beta_2 = \mu_{k-1}^2 + 2y_kC(+1, s_{k-1}^2) - C(+1, s_{k-1}^2)^2$$

$$\beta_3 = \mu_{k-1}^3 + 2y_kC(+1, s_{k-1}^3) - C(+1, s_{k-1}^3)^2$$

$$\mu_k^2 = \max \quad \beta_4 = \mu_{k-1}^0 + 2y_kC(-1, s_{k-1}^0) - C(-1, s_{k-1}^0)^2$$

$$\beta_5 = \mu_{k-1}^1 + 2y_kC(-1, s_{k-1}^1) - C(-1, s_{k-1}^1)^2$$

$$\mu_k^3 = \max \quad \beta_6 = \mu_{k-1}^2 + 2y_kC(-1, s_{k-1}^2) - C(-1, s_{k-1}^2)^2$$

$$\beta_7 = \mu_{k-1}^3 + 2y_kC(-1, s_{k-1}^3) - C(-1, s_{k-1}^3)^2$$

and four best paths:

$$\Gamma_k^0 = +1 \,||\, \Gamma_{k-1}^0 \quad \text{if } \beta_0 > \beta_1$$

$$+1 \,||\, \Gamma_{k-1}^1 \quad \text{else}$$

$$\Gamma_k^1 = +1 \,||\, \Gamma_{k-1}^2 \quad \text{if } \beta_2 > \beta_3$$

$$+1 \,||\, \Gamma_{k-1}^3 \quad \text{else}$$

$$\Gamma_k^2 = -1 \,||\, \Gamma_{k-1}^0 \quad \text{if } \beta_4 > \beta_5$$

$$-1 \,||\, \Gamma_{k-1}^1 \quad \text{else}$$

$$\Gamma_k^3 = -1 \,||\, \Gamma_{k-1}^2 \quad \text{if } \beta_6 > \beta_7$$

$$-1 \,||\, \Gamma_{k-1}^3 \quad \text{else}$$

but:

$$s_{k-1}^i = (\alpha_{k-1}, \alpha_{k-2})$$

$$s_{k-1}^0 = (+1, +1)$$

$$s_{k-1}^1 = (+1, -1)$$

$$s_{k-1}^2 = (-1, +1)$$

$$s_{k-1}^3 = (-1,-1)$$

and:

$$C(+1,s_{k-1}^0) = +1$$

$$C(+1,s_{k-1}^1) = f_1$$

$$C(+1,s_{k-1}^2) = 2f_0 - f_1$$

$$C(+1,s_{k-1}^3) = -f_1$$

$$C(-1,s_{k-1}^0) = f_1$$

$$C(-1,s_{k-1}^1) = f_1 - 2f_0$$

$$C(-1,s_{k-1}^2) = -f_1$$

$$C(-1,s_{k-1}^3) = -1$$

The algorithm again consists of calculating the largest of each metric to each path and piecing together the best path to each state.

No simplifications exist, (for the general case with arbitrary f), although for f = (0.25,0.50,0.25) further simplifications may be made.